2000

Development of an autonomous in situ instrument for stable and precise freshwater pH measurements

Jeffrey J. Carr
The University of Montana

**Maureen and Mike
MANSFIELD LIBRARY**

The University of

Montana

Permission is granted by the author to reproduce this material in its entirety, provided that this material is used for scholarly purposes and is properly cited in published works and reports.

Please check "Yes" or "No" and provide signature

Yes, I grant permission   _____

No, I do not grant permission   _____

Author's Signature: _____

Date: _12/15/00_____

Any copying for commercial purposes or financial gain may be undertaken only with the author's explicit consent.

DEVELOPMENT OF AN AUTONOMOUS IN SITU INSTRUMENT

FOR STABLE AND PRECISE

FRESHWATER pH MEASUREMENTS

By

Jeffrey J. Carr

B.S., Chemistry, The University of Montana, 1998

B.A., Cell and Molecular Biology, The University of Montana, 1998

presented in partial fulfillment of the requirements
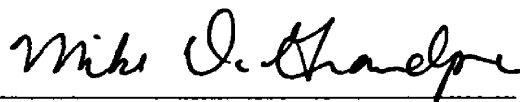
for the degree of

Masters of Science

The University of Montana

2000

Approved by:

_____

Chairperson

_____

Dean, Graduate School

___12_/_20_/_2000___

Date

UMI Number: EP39106

UMI®

Dissertation Publishing

UMI EP39106

ProQuest®

Development of an Autonomous In Situ Instrument For Stable and Precise Freshwater Measurements

Director: Michael D. DeGrandpre

The determination of pH is significant in characterizing and understanding the aqueous equilibrium and kinetics. For example, the CO_2 system can be characterized with equilibrium constants and two of the following parameters, pH, alkalinity, dissolved inorganic carbon, or the partial pressure of carbon dioxide (pCO_2). Changes in the concentration of dissolved CO_2 through biological processes such as photosynthesis and respiration and through physical processes of air-water gas exchange and surface-ground water mixing, are evident in pH. Trace metal speciation and biological processes of lakes and rivers are also dependent on pH. To more effectively study pH variability, a Submersible Autonomous Moored Instrument for pH (SAMI-pH) has been developed. The instrument operates by mixing a sulfonephthalein indicator with a freshwater sample. Once the solutions are mixed, absorbances for the acid (HL^-) and base (L^{2-}) forms of the indicator are collected using spectrophotometric techniques. The SAMI-pH utilizes a 2 cm flow cell, tungsten light source, fiber optics, spectrograph, and microprocessor for collecting data. Laboratory tests have demonstrated a precision of better than ± 0.005 pH units and accuracy relative to another method of ± 0.010 pH units. Testing of the in situ instrument was performed multiple times in the Clark Fork River of the Columbia River Basin near Missoula, Montana.

Development of an Autonomous In Situ Instrument For Stable and Precise Freshwater Measurements

Director: Michael D. DeGrandpre *ﾉｿﾉ ⱴ*

The determination of pH is significant in characterizing and understanding the aqueous equilibrium and kinetics. For example, the CO_2 system can be characterized with equilibrium constants and two of the following parameters, pH, alkalinity, dissolved inorganic carbon, or the partial pressure of carbon dioxide (pCO_2). Changes in the concentration of dissolved CO_2 through biological processes such as photosynthesis and respiration and through physical processes of air-water gas exchange and surface-ground water mixing, are evident in pH. Trace metal speciation and biological processes of lakes and rivers are also dependent on pH. To more effectively study pH variability, a Submersible Autonomous Moored Instrument for pH (SAMI-pH) has been developed. The instrument operates by mixing a sulfonephthalein indicator with a freshwater sample. Once the solutions are mixed, absorbances for the acid (HL^-) and base (L^{2-}) forms of the indicator are collected using spectrophotometric techniques. The SAMI-pH utilizes a 2 cm flow cell, tungsten light source, fiber optics, spectrograph, and microprocessor for collecting data. Laboratory tests have demonstrated a precision of better than ±0.005 pH units and accuracy relative to another method of ±0.010 pH units. Testing of the in situ instrument was performed multiple times in the Clark Fork River of the Columbia River Basin near Missoula, Montana.

Acknowledgments

During my academic stay at The University of Montana I have encountered many wonderful people and made many long lasting relationships. I would like to express my humble gratitude to those people that have assisted and guided me through my graduate education. First and foremost, I would like to thank my advisor Dr. Michael DeGrandpre for his continual support that has given me the opportunity to expand my knowledge both as an undergraduate and graduate student. I would like to acknowledge Matt Baehr for his continual bickering, arguing, and competitiveness for which extended my stay here longer than it should have. In all honesty, he has been of great help to me over the past three years academically and most notably mentally.

I thank Dick Field for his insight with modeling and also Terry Hammar at the Woods Hole Oceanographic Institution for putting up with my continual harassment about electronics and instrumentation problems. I would also like to recognize Jason Reynolds, Cory Beatty, and Shigui Yuan for helping me with the various deployments of the autonomous instrument, discrete sample collection, and performing analyses on samples. Jason has also given me the opportunity to rock climbing for the first time in my life, which by the way was an incredible experience, thanks again for trying to kill me!

I would like to express my appreciation to my entire family for their continual support, specifically my sister Chana, my mother Char, and especially my father Jim, who has made many sacrifices for me to achieve what I have today.

Finally, I would like to show my gratitude to the Department of Chemistry for the educational opportunity and for the greatest opportunity of all, the chance to meet my wonderful and loving wife Glenda (we met in organic chemistry, Spring Semester 1996). She is the best wife and friend that anyone could ever hope for. Through all the trials and tribulations and the long days and nights of my academic endeavors she has stood by me with full encouragement and unwavering love.

Table of Contents

List of Tables

List of Figures

Chapter 1

Introduction

1.1 Literature Review

The title "master variable" has been given to pH due to its importance in aquatic ecosystems. It is defined as the $-\log a_{H+}$ where, a_{H+} is hydrogen ion activity, and is one of the most measured parameters in freshwater. It controls the speciation of the various forms of aqueous inorganic carbon (H_2CO^3, HCO_3^-, and CO_3^{2-}) which creates the buffering capacity of most freshwater environment. The changes in concentration of aqueous CO_2, through biological processes (respiration and photosynthesis) and physical process (mixing of ground water and surface water and air-water gas exchange), are reflected in pH. Determination of pH is therefore critical in understanding aqueous chemical and geochemical processes such as chemical equilibria (Stumm and Morgan 1996), trace metal solubility and speciation (Kramer and Tessier 1982; Herzeg et al. 1985; Psenner 1994), and kinetic processes (Herzeg and Hesslein 1984). The importance of pH is exemplified in its effect on biological activity, where, for example, an acidification of 0.5 pH units can lead to severe consequences for fish populations (Henriksen 1979; Hoenicke et. al. 1991).

Environmental monitoring has become an important contemporary issue throughout the world. Given the expense, time, and sampling constraints associated with typical laboratory analyses, there exists a need for real-time monitoring that is precise, cost-effective, and suited for environmental applications. Increasing environmental regulations and public concern have also resulted in an expanding interest in the

development of in situ sensors. The ability to develop autonomous sensors has been enhanced mainly by improvements in the size and quality of analytical instrumentation as well as advances in fiber optic technologies (Janata et. al 1994). The utilization of autonomous in situ instrumentation eliminates the need for sampling and therefore avoids storage and contamination problems associated with sample collection. It also provides real time analysis, which yields better temporal coverage than is possible with discrete sampling. Autonomous instruments also allow research in areas that are remote and potentially dangerous environments (Angel et al. 1989).

In situ monitoring devices have proven to be useful in a wide variety of environmental applications. They have, for example, been used to study CO_2 cycling in oceanic waters (Hales et al. 1997; DeGrandpre et al. 1997), temperature in deep geothermal wells (Angel et al. 1989), and nitrate in seawater (Jannasch et al. 1994). There have been many different designs ranging from fiber optic based systems like optrodes (Motellier et al. 1993) and evanescent wave spectroscopy (Mizaikoff et al. 1999) to the use of flow injection based instruments (Andrew et al. 1994).

In the case of pH, discrete sampling techniques are very limited in their ability to resolve diel and episodic (run-off from rain or snow or hazardous waste spills) changes in pH. In situ pH instrumentation would provide more extensive data for characterizing natural physical and biological dynamics in aquatic systems. Continuous monitoring would also be very advantageous for studying episodic events. The availability of in situ instrumentation for pH applications is very limited. Most data from the in situ instruments have limited usefulness due to the lack of precision and reproducibility (Ben-Yaakov and Ruth 1973, Maberly 1996).

Although potentiometric methods are commonly the method of choice for freshwater measurements there are several problems associated with their use in low ionic strength and poorly buffered waters. First, no standard protocols have been found that can ensure reproducibility and reliability in interlaboratory, intralaboratory, and field measurements because of electrode error (Gardner et al. 1997). The major sources of error that are commonly found with the use of electrodes in dilute waters are associated with the liquid junction potential. Junction potential errors are caused by a build up of charge, which occurs when ions with different ionic mobility diffuse through the junction (Brezinski 1983). These errors have been found to increase with decreasing ionic strength of the sample solution (Hoenicke et. al. 1991). Some of the common sources of junction potential errors are:

a) Voltage anomalies - there are two commonly observed types:

1) Precipitation of KCl at the liquid junction (this type of anomaly becomes more prominent at lower temperatures)

2) Precipitation of AgCl compounds in KCl solution when it is in contact with low ionic strength samples (Hoenicke 1991, Ozeki et. al. 1998).

b) Calibration using high ionic strength buffers – causes a difference in the liquid junction potentials to be observed when the electrode is used in low ionic strength medium.

As a result of the inherent problems associated with standard glass electrodes there has been a pursuit to find new methods for the determination of freshwater pH. In an earlier investigation, Covington et al. (1983) designed a free-diffusion liquid junction that reduced liquid junction potential errors. Although this method out-performed the

conventional glass electrode by attaining a precision of ±0.01 pH units, drift was still apparent and the apparatus was too cumbersome for field applications.

Another method that has been utilized for more than 100 years is the use of colorimetric indicators in determining aqueous pH. In comparison to potentiometric methods, indicators have a rapid equilibration time, they are more stable over time, and there is no liquid junction potential to worry about. Traditional colorimetric methods have used pH kits, which depend on visual determination of pH against a color scale. These methods have demonstrated a poor accuracy of ±0.2-1.2 pH units based on comparisons with potentiometric readings (Haines 1983). A flow injection instrument, based on a multi-indicator system (Pia et. al. 1990) for freshwater applications, was reported to have reproducibility from ±0.07 to ±0.14 pH units. This method showed an improvement over traditional visual colorimetric methods because the method used spectrophotometric measurements. The low precision resulted from measurements at a single wavelength, which are both concentration and pathlength dependent.

Over the past 20 years, advances in analytical methodology, instrumentation, and environmental concern have fostered vast improvements in techniques for determination of seawater pH (Robert-Baldo et al. 1985, Byrne 1987, King and Kester 1990, Bellerby et al. 1995, Sedjil and Lu 1998). A precision of better than ±0.0003 pH units (Clayton and Byrne 1993) and an accuracy of ±0.001 pH units (Millero et al. 1993) has been achieved when using indicators and spectrophotometric techniques. The major contributor to the advancement of the colorimetric methodology was from the research done by Robert Byrne and colleagues. The methodology involves measuring the absorbance of an

indicator at two different wavelengths. The ratios of the two absorbances (base/acid) are obtained, which is then independent of concentration and pathlength.

Unlike seawater methods, improvements in the measurement techniques for freshwater have not materialized. French (1999), a previous M.S. student of Dr. Michael DeGrandpre, has investigated the development of an automated pH system utilizing the "Byrne Method" for freshwater applications. The benchtop pH system achieved a relative accuracy of ±0.008 pH units (when compared to an UV-VIS spectrophotometer) and a precision of ±0.001-0.004 pH units.

A problem associated with pH indicators is that they are weak acids, so when they are implemented for freshwater analyses they may alter the observed pH of a sample. The use of a single indicator dye is also limited to a set pH range, which is ±1 pH unit from the pK_a of the indicator of choice.

1.2 Research Objectives

The research goal is to improve and expand upon the work done by French (1999), with the objective to build and deploy an autonomous in-situ pH instrument for monitoring freshwater pH. The French (1999) system however had various shortcomings (slow response time, extended flush time and extensive power consumption) which required further modifications to be practical for in situ applications. To achieve this goal, an evaluation of the pH indicator for freshwater conditions was conducted. Then modifications to the laboratory design, measurement cycle, power consumption, and the response and flush time were performed, which ultimately lead to development of a

stable and precise submersible autonomous moored instrument for determination of freshwater pH (SAMI-pH).

In the following chapters I will first describe the methods that were utilized in building, optimizing, deploying, and verifying the performance of the autonomous instrument. Then the results from laboratory and river studies will be presented, followed by a discussion and conclusion of the resulting data.

Chapter 2

Operating Principle

2.1 Theory of the Byrne Method

It is necessary to first review the Byrne method to understand the design and operation of the autonomous in situ instrument. The theory is based on the acid-base characteristics of a weak acid indicator,

$$HL^- \rightleftharpoons H^+ + L^{2-} \tag{1}$$

where HL^- is the protonated or acid form of the indicator, L^{2-} is the deprotonated or base form of the indicator (the sulfonephthalein-type indicators we use are diprotic, but the H_2L form only exists near a pH of 1.5). Based on the condition stated in Equation (1) the equilibrium relationship is:

$$K_a = \left(\frac{[H^+][L^{2-}]}{[HL^-]} \right) \left(\frac{\gamma_{H^+} \gamma_{L^{2-}}}{\gamma_{HL^-}} \right) \tag{2}$$

where [ ] denotes concentration, and γ represents the ion activity coefficients of the individual species. Taking the -log of Equation (2) yields the Henderson-Hasselbalch equation,

$$pH = pK_a + \log \left(\frac{[L^{2-}]}{[HL^-]} \right) + \log \left(\frac{\gamma_{L^{2-}}}{\gamma_{HL^-}} \right). \tag{3}$$

7

Equation 3 can be combined with Beer's Law,

$$A_\lambda = \varepsilon_\lambda bc \qquad (4)$$

where ε_λ is the molar absorptivity of indicator at wavelength λ, b is the optical pathlength, c is the concentration of indicator solution in the optical cell, and A_λ is the absorbance at wavelength λ, to derive an equation for pH as a function of temperature and indicator absorbance ratio. The equation is represented as:

$$pH = pK_a{}' + \log\left(\frac{R - e_1}{e_2 - Re_3}\right) \qquad (5)$$

where R is the ratio of absorbance maxima for the acid (λ_1, $\sim$ 439 nm) and base (λ_2, $\sim$ 577 nm) forms ($A_{\lambda2}/A_{\lambda1}$) and the temperature dependant variables are the $pK_a{}'$, which is the apparent dissociation constant that includes the γ term in Equation 3 and the molar absorptivity ratios (e_1, e_2 and e_3) of the acid and base forms:

$$e_1 = \frac{\varepsilon_{a577}}{\varepsilon_{a439}} \qquad e_2 = \frac{\varepsilon_{b577}}{\varepsilon_{a439}} \qquad e_3 = \frac{\varepsilon_{b439}}{\varepsilon_{a439}}. \qquad (6)$$

The autonomous instrument operates by collecting intensities, which are then converted, into absorbances by,

$$A_\lambda = -\log(I_\lambda / I_{\lambda o}) \qquad (7)$$

where I_λ is the intensity transmitted through the indicator/sample solution and $I_{\lambda o}$ is the instensity transmitted through the blank solution (water sample).

To utilize the operating principle for freshwater applications the e's will had to be obtained as a function of tempertature. Once the e's were found, the pK_a' could then be determined using a low ionic strength solution. After the indicator was characterized, the autonomous instrument was be constructed and optimized (plumbing, response time, optics, the indicator mixing, and pH perturbation) to collect intensities.

Chapter 3

Methods

3.1 Indicator Characterization

An appropriate indicator should be used that has a pK_a' within approximately ± 1 pH unit of the aquatic system that is to be monitored. The proposed study site, the Clark Fork River of the Upper Columbia River Basin near Missoula, Montana, was determined to have an approximate pH of ~8.6 to 7.8 (French 2000). This led to the use of the sodium salt of cresol red with a pK_a' of ~8.20 ± 0.05 at 20 °C (Kolthoff 1930) (Figure 3.1).
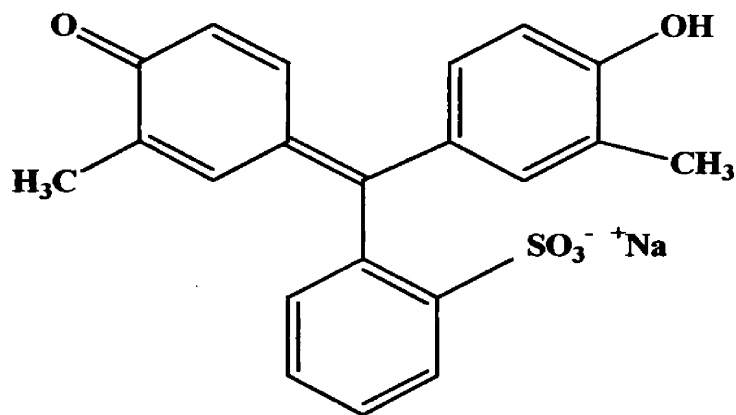
Figure 3.1. 2-dimensional molecular structure of cresol red (sodium salt).

3.1a Determination of Molar Absorptivities

The molar absorptivities of the pH indicator cresol red, have been determined to be a very weak function of temperature (Robert-Baldo et al 1985). A previous determination of the molar absorptivities was done at a single temperature of 20.0°C

10

(French 1999). Due to fluctuations in the seasonal water temperatures, typically as low as $0\ ^{\circ}C$ during the winter and greater than $15^{\circ}C$ in the summer, the determination of the molar absorptivities as a function of temperature is critical in obtaining a more accurate pH.

To determine the molar absorptivities, the indicator had to be converted into its monoprotic and fully deprotonated forms. A buffer of pH 4 was chosen so that the fully protonated (present at a pH < 3) and the fully deprotonated (present at a pH > 7) forms of the indicator would be excluded, leaving the indicator exclusively in the singly protonated form. The pH 4 solution was prepared by adding potassium hydrogen phthalate (dried for 1 hr @ $110^{\circ}C$) to 1 kg of HPLC grade deionized (DI) water (Fisher Scientific). The pH 12 solution was prepared by dissolving 0.400 g of sodium hydroxide into 1 kg of DI water.

Measurements were made using a UV-VIS spectrophotometer (Perkin-Elmer, Lambda 11) equipped with a 1 cm thermostated cell holder. The cell holder was temperature controlled by a bath/circulator (NESLAB, RTE-111). Due to temperature fluctuations from the water bath to the cell holder, an external digital temperature probe (HH64 Thermistor, Omega Engineering Corp.) with a reported accuracy of $0.1^{\circ}C$ was used to monitor the water temperature exiting from the cell holder. The temperatures were then adjusted in the water bath so that the external thermistor displayed the desired temperature. Temperatures of 20, 15, 10, 8, and $5^{\circ}C$ were used during the experiment.

The test samples were prepared by adding 1.008×10^{-2} mol kg^{-1} cresol red solution to a portion of the acid and the base buffer resulting in a concentration of 1.795×10^{-5} mole kg^{-1}. Initially, a blank (buffer without indicator) was run at the beginning of the

temperature test and then the cuvet was filled with the indicator/buffer solution. The sample solution was then equilibrated at each temperature and an absorbance spectrum was collected from 700 nm to 350 nm. Once the spectra were collected, another blank was run at the last temperature measurement to compensate for any instrumental drift. This procedure was repeated three times for each of the buffer solutions over the full temperature range. Figure 3.2 represents the averaged absorbance data that were collected and used in determining the molar absorptivities and ultimately the molar absorptivity ratios (Equation 6).
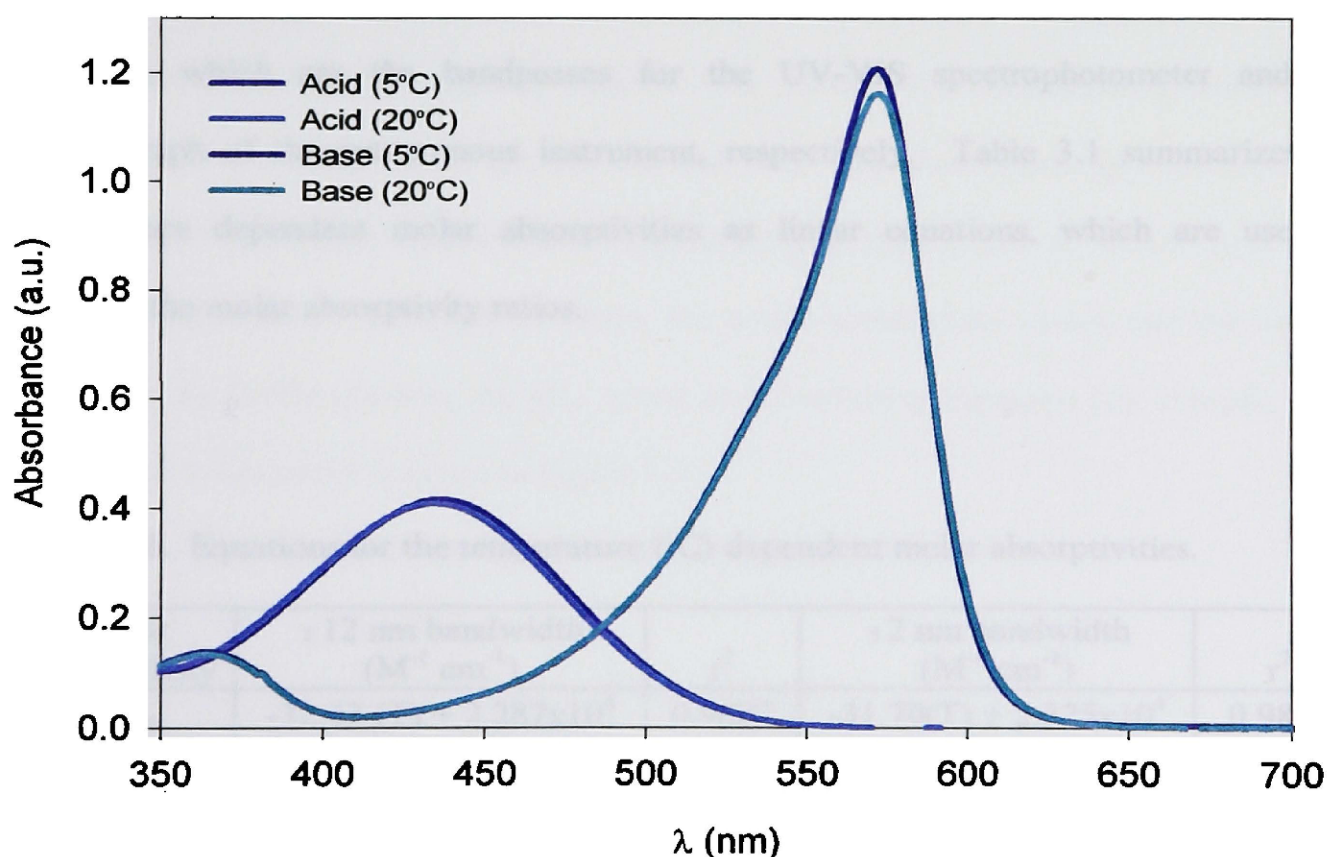
Figure 3.2. Absorbance spectra of the cresol red indicator in a basic solution (with a peak at ~573 nm) and in an acid solution (with a peak at ~435 nm). Concentrations for both solutions were 1.795×10^{-5} mole kg^{-1}.

The absorbance from the molar absorptivity test demonstrates very weak dependence of temperature by the acid form of the indicator. The basic form of the cresol red indicator exhibits a stronger dependence on temperature (Figure 3.2) with a decrease of about 0.030 absorbance units (a.u.) from the 5°C trial to the 20°C trial. Therefore the temperature dependence is significant and must be incorporated into the pH calculation.

The resulting absorbances, pathlength, and indicator concentration were used in the Beer's Law equation to determine the molar absorptivities as function of temperature at the 439 nm and 577 nm (the basis for selecting these two wavelengths will be discussed later in the chapter). The absorbances were averaged over a range of ±2 and ±12 nm, which are the bandpasses for the UV-VIS spectrophotometer and the spectrograph of the autonomous instrument, respectively. Table 3.1 summarizes the temperature dependent molar absorptivities as linear equations, which are used to compute the molar absorptivity ratios.

Table 3.1. Equations for the temperature (°C) dependent molar absorptivities.

Molar Absorptivity	±12 nm bandwidth (M^{-1} cm^{-1})	r^2	±2 nm bandwidth (M^{-1} cm^{-1})	r^2
ε_{a439}	-32.43 (T) + 2.287x10^4	0.9887	-31.70(T) + 2.325x10^4	0.9851
ε_{a577}	<1	NA	<1	NA
ε_{b439}	9.676 (T) + 2.179x10^4	0.9713	11.60(T) + 2.108x10^4	0.9854
ε_{b577}	-47.69 (T) + 5.596x10^4	0.9988	-111.5(T) + 6.435x10^4	0.9991

3.1.b pK$_a$ Determination

With the temperature dependence of the molar absorptivities determined, a more accurate pK$_a$' (free of the ε's temperature dependence) could be determined. The pK$_a$' was characterized by using a low ionic strength buffer with a known pH as a function of temperature (5 - 25°C). The low ionic strength buffer (0.01 M) was prepared by dissolving 0.1183 g of KH$_2$PO$_4$ and 0.4320 g of Na$_2$HPO$_4$ (both reagents were dried for ~1 1/2 hrs @ 120°C) in 1 kg of degassed DI water (Covington et al. 1983). The pH of this buffer is 7.621 at 20 °C. This experiment utilized the same instrumental setup as described for the molar absorptivity experiment.

Initially, a blank was run using the buffer solution. To the blanked buffer, 80μl of the 1.008x10^{-2} mole kg^{-1} cresol red solution was added. The solution temperature was then allowed to equilibrate to 20, 15, 10, and 5°C. An absorbance measurement was collected for each of the equilibration temperatures, by which then R values (A$_{577}$/A$_{439}$) could be determined. With the R values, the molar absorptivity ratios, and the known pH's from the buffer solution, the pK$_a$' could be solved using Equation (5). The pK$_a$' as a function of temperature is given in Figure 3.3.

The data were fit to the equation (Ramette et al. 1977):

$$pK_a' = \frac{A}{T} + B + C \log T \tag{8}$$

where T is the temperature in Kelvin and A, B, and C are thermodynamic constants. The determination of he thermodynamic constants was performed using a nonlinear least squares analysis (Sigma Plot, SPSS Inc.).
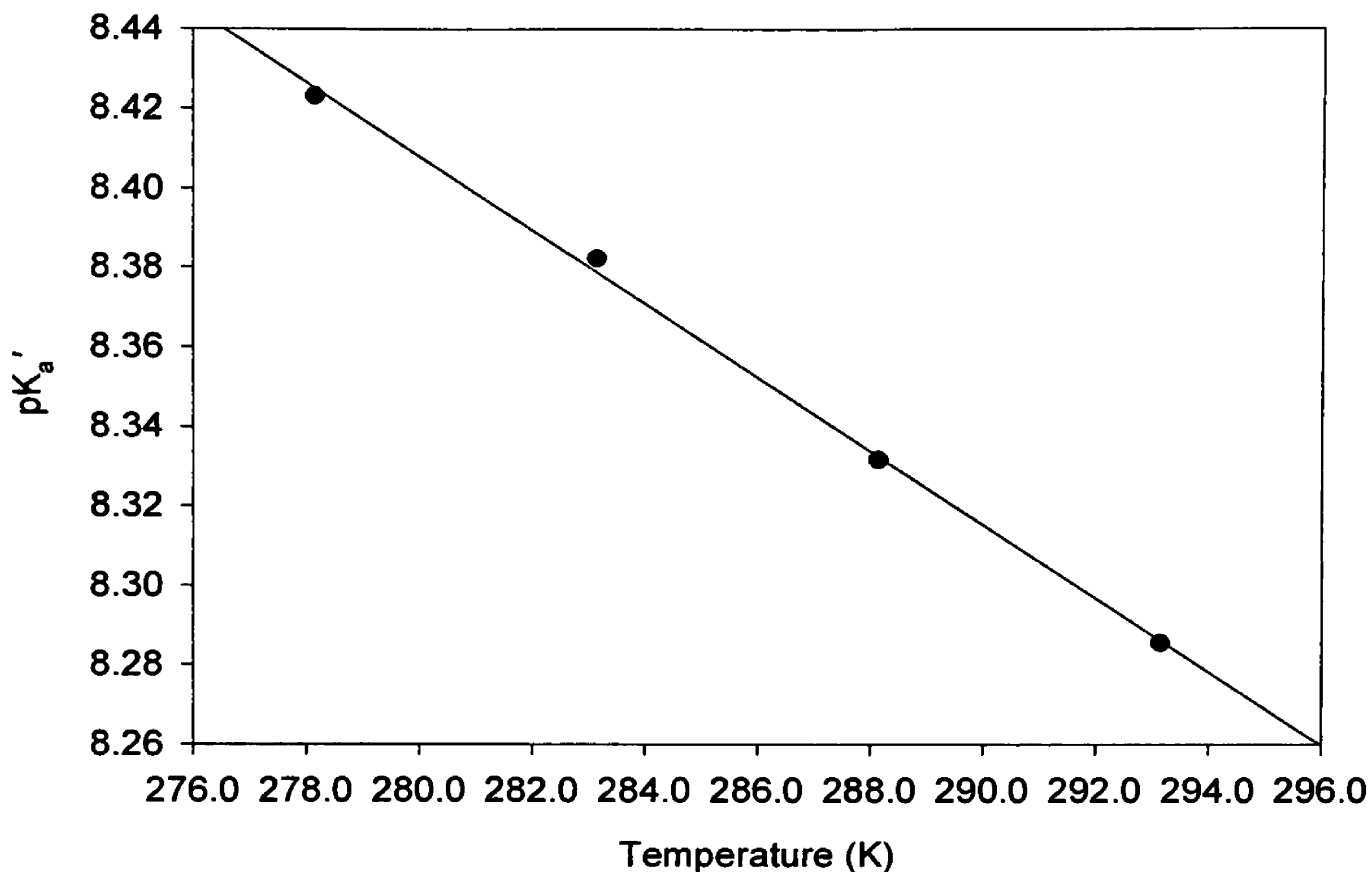
Figure 3.3. The determination of cresol red pK_a' as a function of temperature using a low ionic strength buffer. The line represents the linear regression with a $r^2 = 0.9999$.

The results of the analysis produced the following equation for the pK_a':

$$pK_a' = \frac{913.4}{T} + 2.049 + 1.266\log T. \tag{9}$$

The ability to accurately measure pH is directly linked with the accuracy of the pK_a'. Even though the pK_a' trials gave a reproducibility of ±0.001 (N=3), the overall accuracy is limited to ±0.01 pH units due to the accuracy of the buffer pH (Covington et al. 1983).

It is important to note that the pK_a' was quantified using a solution that was of higher ionic strength ($\mu = 0.01$ M) than that of typical fresh water environments ($\mu <$

0.005 M). Because of the activity coefficients in Equation 3, the difference in ionic strength causes a salt error to be observed in the calculated pH (Kolthoff 1928). Due to the inability to calculate the effective hydrated radius of the indicator the activity coefficients in Equation 3 can not be determined using the extended Debye-Huckel equation. If the hydrated radius for cresol red can be calculated, a correction for the salt error could be applied for the differences in the ionic strength between the buffer and the freshwater sample. Although the accuracy of the pK_a' and its ionic strength dependence needs to be improved, this does not alter the ability to compile accurate and reliable absorbance data. Absorbance measurements free from random or systematic error will always be valid because they are only dependent on the thermodynamic properties of the indicator. Therefore, a more accurate determination of the pK_a' will only facilitate a more accurate determination of pH.

3.2 Construction of SAMI-pH

The construction of the SAMI-pH instrument utilized a combination of new and pre-existing parts. The pre-existing parts were obtained from an autonomous CO_2 sensor (the Submersible Autonomous Moored Instrument for CO_2 or SAMI-CO_2) (DeGrandpre et al. 1995) and the prototype benchtop pH instrument (autonomous laboratory pH instrument or ALpHI) designed by French (1999). The basic strategy used when constructing the instrument was to make the system resemble a flow injection system. That is, there would be a continuous carrier stream (water sample) to which indicator would be injected. The carrier stream would then mix and be transported to an optical flow cell where measurements would be performed. The proposed system only differs

from a flow injection system by utilizing multiple pulses of sample instead of a continuous flow.

3.2.a Conversion of Old SAMI-CO₂

The development of the SAMI-pH was greatly facilitated by the use of many of the components from the SAMI-CO$_2$ system. The major components are shown and labeled in Figure 3.4. Materials used from the existing SAMI-CO$_2$ to build the SAMI-pH were the main pressure housing, the external pump and valve housing, and the electronics. The main pressure housing consists of a 61 cm length of 6" ID PVC pipe that is sealed on both ends with o-rings to make a waterproof seal. The top end cap is also attached to the internal bracketing, to which all of the internal components are fastened. The top end cap also supports the external pump and valve housing. The pump and valve housing is constructed out of a 2" ID PVC tubing with a length of 10.2 cm. One end is sealed with an o-ring fitted end cap and the other end utilizes a rubber diaphragm to equalize the hydrostatic pressure, thus allowing the pump and valve to operate properly underwater.

Other components that were also adapted from the CO$_2$ instrument are the data logger (TattleTale 4A, Onset Computer Corporation), internal electronics (clock board, voltage regulator, and wiring), and spectrograph (American Holographics Inc., MS10). A custom designed 1.8 cm flow cell and 600 μm core fiber-optics (F-MSC-OPT, Newport Corporation) were used from the AlpHI.
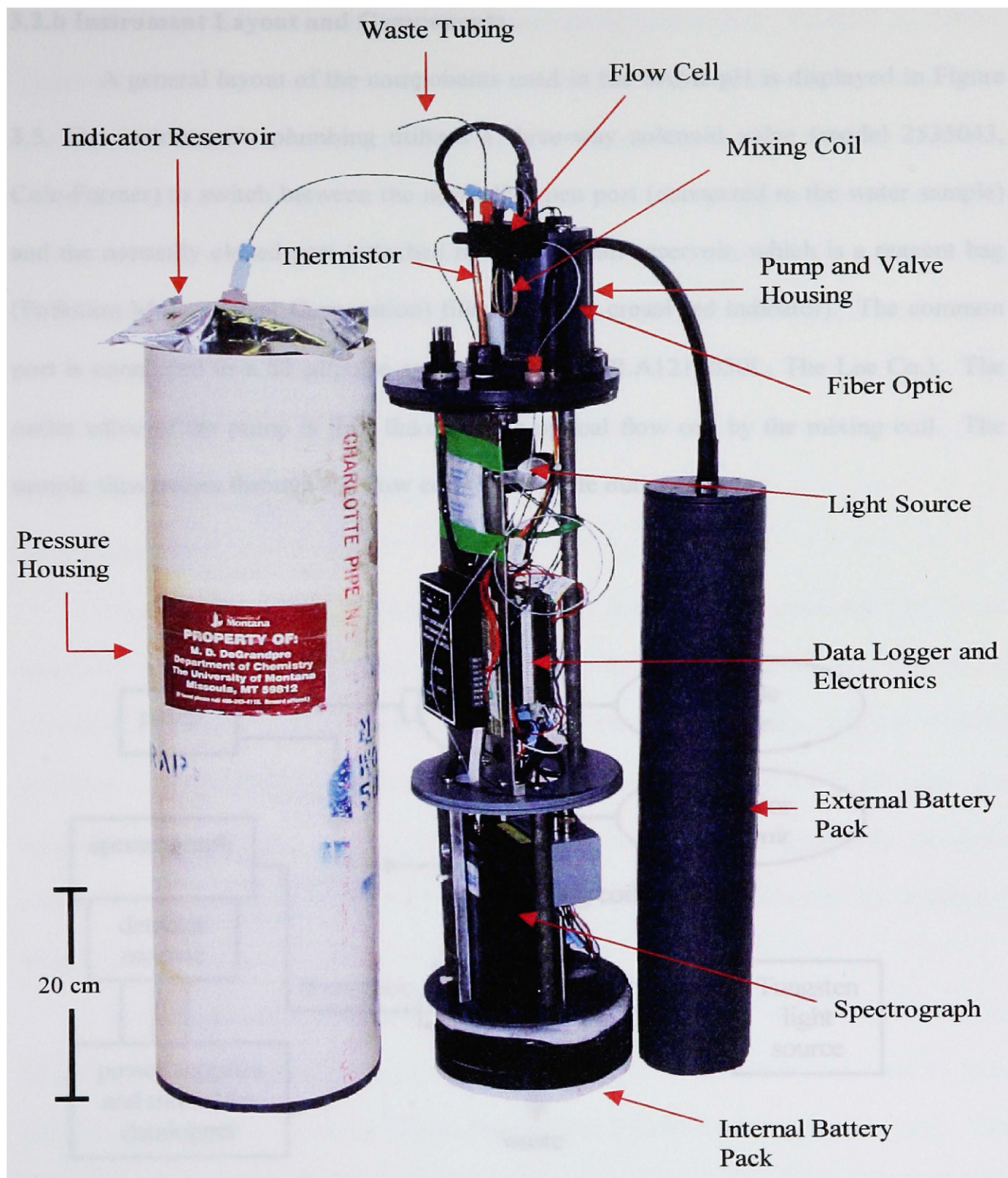
Figure 3.4. The SAMI-pH, with major operating components labeled.

3.2.b Instrument Layout and Components

A general layout of the components used in the SAMI-pH is displayed in Figure 3.5. The instrument's plumbing utilizes a three-way solenoid valve (model 2535043, Cole-Parmer) to switch between the normally open port (connected to the water sample) and the normally closed port (attached to the indicator reservoir, which is a reagent bag (Pollution Measurement Corporation) filled with the cresol red indicator). The common port is connected to a 50 μl/pulse solenoid pump (LPLA1210050L, The Lee Co.). The outlet valve of the pump is then linked to the optical flow cell by the mixing coil. The sample then passes through the flow cell to the waste outlet.
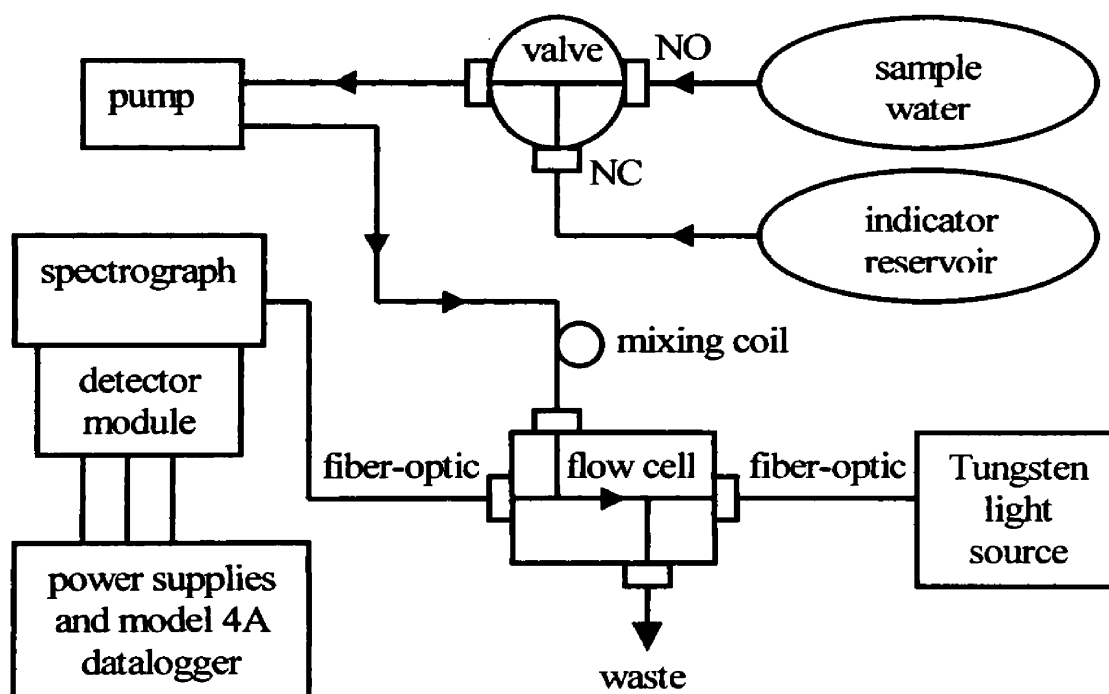
Figure 3.5. A schematic of the SAMI-pH components (NO = normally open, NC = normally closed) (French, 1999).

The optical system consists of a tungsten light source (5 V, 0.12 A, Gilway Technical Lamps) with output transmitted to the flow cell via the 600 μm core fiber-optic. The resulting attenuated light is captured on another section of fiber-optic and propagated to the spectrograph. The light is dispersed by the spectrograph onto three photodiodes located at 439, 577, and 735 nm. The detected voltages are converted into digital signals and stored in the data logger, which are used later in the calculation of pH.

3.3 Instrument Optimization

3.3.a Plumbing

When constructing the SAMI-pH a few response characteristics had to be addressed to ensure that the instrument would be functional as an in situ instrument. Essential instrument characteristics include good long-term stability, a good working precision ($\pm$0.005 pH units or better), a relative accuracy better than $\pm$0.01 pH units, low reagent and power usage, and the ability to sample in a short time period (fast response time). The following optimizations of SAMI-pH will be in reference to the bench-top ALpHI instrument developed by French (1999).

The ALpHI design used a 152 cm length of 0.007" ID tubing to create backpressure in the optical flow cell (Figure 3.5). The backpressure was used to force bubbles into solution, therefore eliminating optical interferences in the flow cell. This however, made the sample flow rate very slow (~2 minutes for every 50 μL pulse). The ALpHI also used a 152 cm length of 0.040" ID tubing coiled up to serve as the mixing coil. With this length of coil it would take ~ 1 hour for a full pulse (50 μl) of indicator or

water sample to travel from the pump to the optical flow cell. Thus, for the ALpHI to obtain data in a reasonable rate of time, the amount of indicator injected into the plumbing had to be controlled by a long length (~1 m) of restriction tubing (.010" ID) and a 1 ms pump pulse of indicator. The indicator pulse was then followed by a 50 µl pulse of sample water and the cycle was repeated. The restriction tubing and quick indicator pulse resulted in inconsistent pump performance and a slow response time.

The sole purpose of the design and layout of the ALpHI was to eliminate the problem of bubbles forming in the flow cell. To minimize the problem of bubble formation in the optical flow cell, changes were made to the plumbing and the indicator and in-lab sample preparation. The first step in bubble reduction was to replace all of the Teflon tubing (with the exception of the tubing to and from the pump, due to incompatibility with the pump fittings) with non-gas-permeable PEEK tubing. In addition, all solutions were degassed under a vacuum and were transferred into reagent bags gravimetrically to minimize gas uptake.

The original exit tubing was replaced with a 13.5 cm length of 0.040" ID tubing. The next improvement was the removal of the restriction tubing that ran from the indicator reservoir to the valve. The tubing was replaced with a larger diameter tubing (0.030" ID). This permitted the pump to deliver a full 50 µl pulse. By reducing the length and increasing the diameter of the restriction and back-pressure tubing, the flow rate of the 50 µl pulse increased from ~2 minutes to ~1 second.

Now that the indicator and sample could be pulsed rapidly through the plumbing, changing the length of the mixing coil was required to further optimize the SAMI-pH. The original 152 cm length of tubing required the pump and the valve to be activated 25

times to transport the sample through the mixing coil. This increased the response time and consumed large quantities of power. To optimize the mixing of a freshwater sample and the indicator, many different lengths of 0.040" ID mixing coils were tested. If the tubing was too long (over 100 cm), too much power was consumed to pump the sample through the excess length. If the mixing coil was too short (less than 10 cm), the indicator and the water sample would not mix adequately. Through trial and error, a length of 24 cm 0.040" ID PEEK tubing was found to give optimal mixing along with minimal pumping.

The response time enhancements resulted in the ability to rapidly pulse indicator and water samples. At the same time, rapid flow rate and tubing volumes did not reduce the ability of the instrument to extract bubbles. The SAMI-pH now operates by drawing a 50 μl pulsing of indicator followed by a number of sample pulses. The response time for a measurement and blank cycle for the ALpHI was 50 and 80 min., respectively. The optimizations to the SAMI-pH have reduced the measurement and blank cycles to ~ 2 and 5 minutes, respectively.

3.3.b Optical System

The major optical components of the SAMI-pH will now be discussed in more detail. The SAMI-pH utilizes two 1 m sections of 600 μm core fiber optic. Great care is taken so that the ends of the fibers are cleaved at a right angle resulting in a flat and smooth surface. The light propagating through the fiber optic is dispersed by the spectrograph and collected by one of the three photodiodes. The spectrograph was fitted with a plastic plate (Figure 3.6) with holes in it to accommodate the three diodes used in the instrument. The linear reciprocal dispersion of the spectrograph (10 nm/mm) was
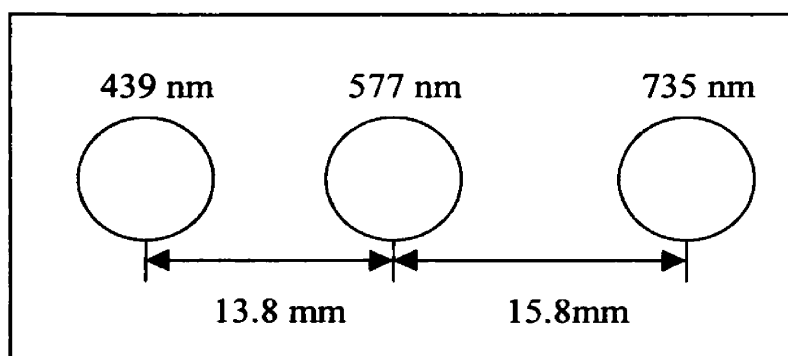
Figure 3.6. The diode spacing on the plate used in the SAMI-pH.

used to determine the distance for holes in the diode plate. As stated earlier, the peak wavelengths for the acid and base form the cresol red indicator is 435 nm and 573 nm, respectively. Due to availability and inexpensive cost of a 577 nm bandpass filter, the spectrograph is calibrated (described in the next section) at 577 nm to measure the base form of the indicator. The hole for the 577 nm diode was drilled in the center of the plate. Based on the reciprocal linear dispersion of the spectrograph's grating, a distance from the 577 nm channel can be calculated for the placement of the 439 channel and the 735 nm channel. For the SAMI-pH diode plate, holes were drilled 13.8 mm and 15.8 mm, respectively away from 577 nm diode hole. These distances resulted in 439 nm for channel and 735 nm for the reference channel.

A GaP photodiode (G-1962, Hamamatsu Corp.) with a peak sensitivity of 440 nm was used for the acid channel and the other channels were fitted with a Si photodiode (S-2386-5K, Hamamatsu Corp.) with peak sensitivities of 960 nm.

3.3.b.1 Wavelength Calibration

The following method was performed to calibrate the SAMI-pH spectrograph at 577 nm. First, the spectrograph was attached to a light source via a length of the 600 μm core fiber optic. The detector power to the photodiodes was turned on. A multimeter (Fluke, 87 III True RMS) was attached to the 577 nm channel to measure the resulting light intensities. Then, the 577 nm bandpass filter (577FS05-25, Andover Corporation) was placed in front of the light source and covered with black cloth to eliminate stray light from outside sources. The grating of the spectrograph was then adjusted so that the maximum intensity was observed on the multimeter. Once the maximum intensity was determined the grating is locked into place. Because the distance between the photodiodes is set, the other two channels are simultaneously calibrated when the 577 nm channel is calibrated.

3.3.b.2 Stray Light Determination

The same set up used in the wavelength calibration of the spectrograph was also used for the determination of stray light. Scattering from dust particles, grating scattering, and reflections from the spectrograph walls are all possible sources of stray light, which can affect the photometric accuracy of the autonomous instruments spectrophotometric measurements (Ingle and Crouch 1988). The procedure for the determination of stray light first involves the acquisition of a dark measurement (this is with the light source turned off). A raw light intensity was then measured (with light on), followed by collection of an intensity when a long pass filter is put in front of the light source. A 700 nm and a 600 nm long pass filter (Andover Corporation) were used in the

measuring of stray light at the 577 nm and 439 nm channels respectively. Stray light is determined by the following equation:

$$\%\text{Stray Light} = \frac{I_{Filter} - I_{Dark}}{I_{Raw} - I_{Dark}} \times 100. \tag{11}$$

Stray light for the optical system should be less than 0.1%. Stray light for SAMI-pH at the 439 (the GaP photodiode is insensitive to IR) and 577 channels were 0.00 % and ~30.00 % respectively. Using a combination of filters it was determined that the stray light was infrared emission from the tungsten light source. To correct this problem the 577 nm channel S-2386-5K diode with a peak intensity of 960 nm was replaced with a G1126-02 diode, from Hamamatsu Corporation, with a peak intensity of 610 nm and a spectral range of 190 nm to 680 nm. This new photodiode reduced the stray light at the 577 nm channel to 0.00 %.

3.3.b.3 Absorbance Accuracy of the Spectrograph

After the stray light was reduced, the absorbance accuracy could then be addressed. Neutral density filters, of 0.1 a.u. and 0.2 a.u. with a tolerance of 10%, were used to determine the absorbance accuracy of the SAMI-pH. The absorbance determined on the UV-VIS (Varian, Cary Bio 300) was used as a reference for the SAMI-pH spectrograph. The absorbance filter was determined with the UV-VIS using,

$$A_{Test} = A_{0.2} - A_{0.1} \tag{12}$$

where $A_{0.2}$ and $A_{0.1}$ are the absorbances for the 0.2 and 0.1 neutral density filters.

With rearrangement of Equation 12, A_{Test} for SAMI-pH can be calculated by,

$$A_{Test} = -\log\left(\frac{I_{0.2}}{I_{0.1}}\right)$$ (13)

where $I_{0.2}$ and $I_{0.1}$ are the intensities for the 0.2 and 0.1 neutral density filters. Although the difference in A_{Test} results between the SAMI-pH and the UV-VIS was very small, it is still of significance (N = 3) (Table 3.2). The standard deviation for the SAMI-pH equates into a maximum pH change of ± 0.028 pH units. The error associated with the SAMI-pH measurements was in the placement and positioning of the filter in front of the light source. The absorbance accuracy is determined using his method because the reflection off the filter in the SAMI-pH is different than the UV-VIS. This is due to the angular output of the fiber. By taking the difference between the two filters, the differences in reflection between the two methods is eliminated.

Table 3.2. Absorbance accuracy results using 0.1 and 0.2 neutral density filters.

		SAMI-pH		UV-VIS	
		A_{Test} (439 nm) (N = 3)	A_{Test} (577 nm) (N = 3)	A_{Test} (439 nm) (N = 3)	A_{Test} (577 nm) (N = 3)
Absorbance	Avg.	0.082	0.093	0.080	0.089
	Std. Dev.	0.004	0.003	0.001	0.001

3.4 Measurement Cycles

The collection of pH data by the SAMI-pH is performed by two separate measurement cycles, the blank measurement cycle and the pH measurement cycle. The two cycles are operated by the pHV3.TT4 program (Appendix 1). A typical measurement cycle consists of collecting time, date, temperature, and intensities for the three wavelengths.

3.4.a Blank Measurement Cycle

To calculate the absorbances for the SAMI-pH at 439 and 577 nm, $I_{\lambda o}$ must be determined for a blank sample. Due to the significant consumption of power and time the instrument is programmed to run a blank measurement only twice per day. The blank cycle flushes the indicator from the plumbing and optical flow cell with 100 pulses of water, which is ~5 ml of sample water (68 from the blank cycle and 32 from the prior measurement cycle) (Figure 3.7). Once the 100 pulses of water are finished, the intensities from the 439, 577, and the 735 channels are recorded. The intensities are then used to determine the blank constants (K_{439} and K_{577}) which will be used in the calculation of absorbances between blank measurements. The K's are determined as follows:

$$K_{439} = \frac{I_{439}}{I_{735}} \quad \text{and} \quad K_{577} = \frac{I_{577}}{I_{735}} \tag{14}$$

where I_{439}, I_{577}, and I_{735} are the intensities at 439, 577, and 735 nm, respectively.
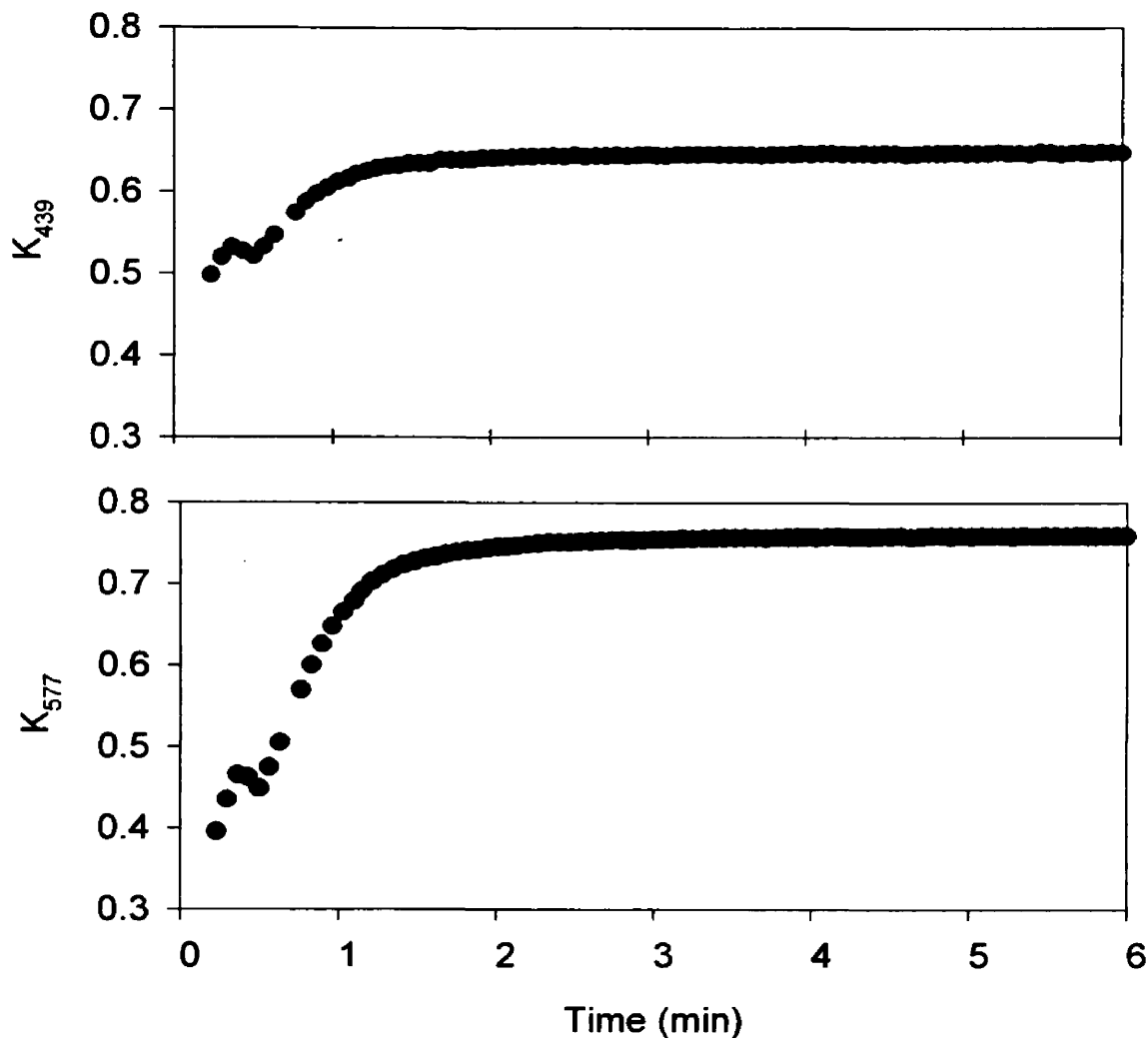
Figure 3.7. The blank constants K_{439} and K_{577} shows that it takes approximately 4 minutes to flush the indicator out of the plumbing.

The blank constants for the 439 and 577 nm channel (Figure 3.8A and B, respectively) collected during a deployment in the Clark Fork River in October of 2000 demonstrate a dependence on temperature (Figure 3.8D). As the temperature decreases the calculated blank constants also decrease. The substantial magnitude differences observed in both the 439 and the 577 nm channel over the duration of the test period demonstrates the need for frequent blank constant determination during testing periods of large temperature variability.
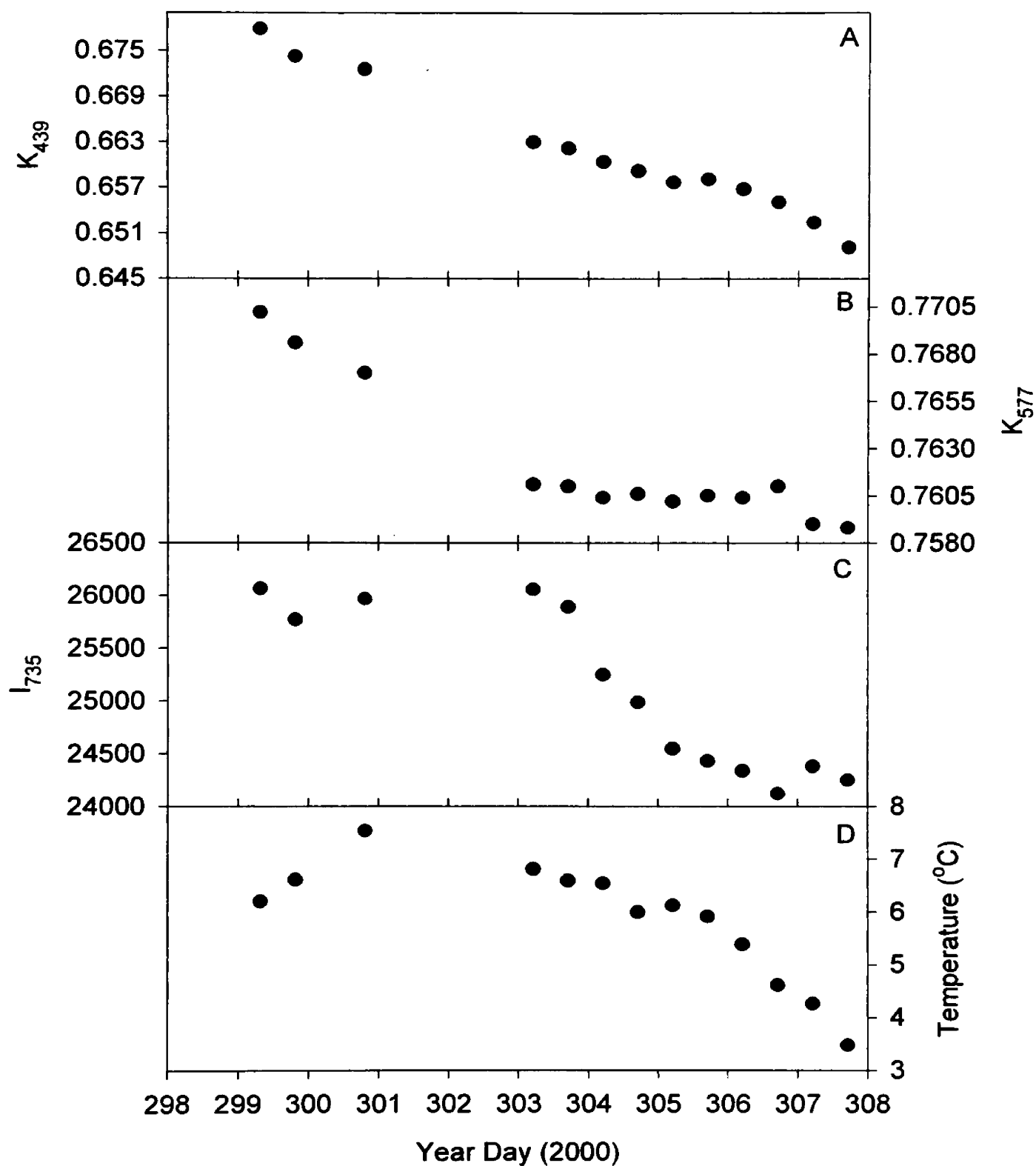
Figure 3.8. Calculated blank constants for the 439 (A) and 577 nm (B) channels, intensities for the 735 nm channel (C), and temperature (D) for collected during a deployment in the Clark Fork River (October 2000).

3.4.b pH Measurement Cycle

For pH to be calculated, the R (A_{577}/A_{439}) must be determined. The optical absorbances at 439 and 577 nm can be calculated using,

$$A_\lambda = -\log\left(\frac{I_\lambda}{I_{ref}K_\lambda}\right) \qquad (15)$$

where A_λ is the sample absorbance at wavelength λ, I_λ is the intensity transmitted through the sample, K_λ is the blank constant for the most recent blank measurement cycle, and I_{ref} (I_{735}) is the transmitted intensity at a wavelength where the indicator does not absorb. I_{735} is used to correct for intensity fluctuations from the source or transmittance in the optical system that may occur between absorbance measurement. Once the absorbances for the acid and base forms are calculated the R value can be computed and used in Equation 5 to calculate pH.

A pH measurement using the SAMI-pH consists of three sequences. First, there is an initial 50 µl pulse of the cresol red solution (2.0×10^{-2} mole kg^{-1}). Second, the indicator slug is transported through the plumbing to the optical flow cell by 18 rapid pulses of sample water. Finally, the detectors and light source are turned on and intensities for the three wavelengths are recorded for 14 water pulses. For the SAMI-pH, the 18 and 14 pulse combination was used so absorbances between 0.09 and 1.00 a.u. would be collected. By changing of the measurement cycle to a full pulse of indicator, it was assumed that pH measurements could be collected near the tail end of the slug where the indicator would mix with the ensuing water pulses. This change led to a very interesting observation in the output intensity at the 735 nm channel. The intensity
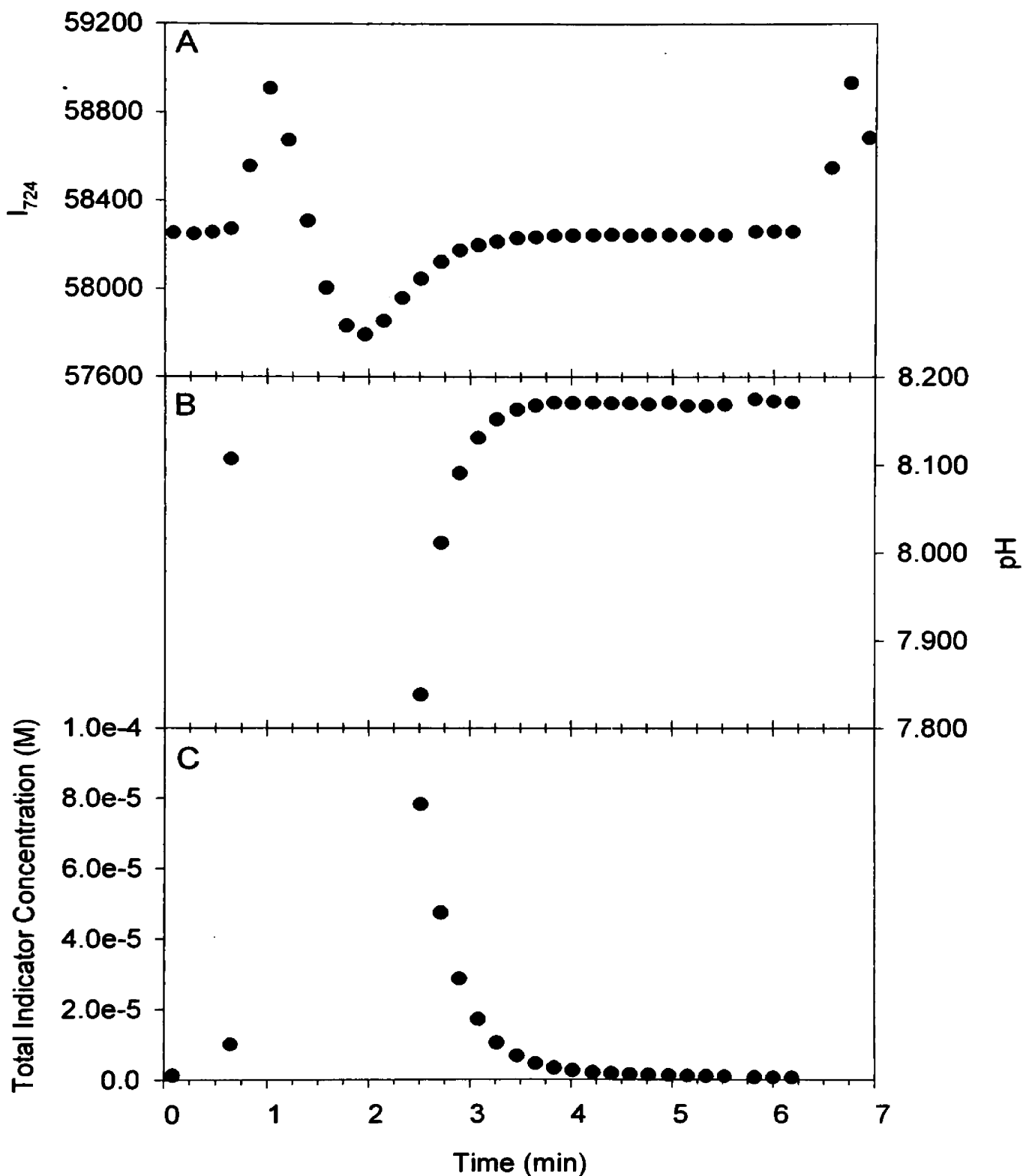
Figure 3.9. This figure demonstrates how the reference intensity (A) and the pH change as a 50 μL indicator slug passes through the optical flow cell. The test was run using a buffer with a pH of ~8.2.

fluctuated as the slug of indicator passed through the flow cell (Figure 3.9A). As the highly concentrated indicator slug passes through the optical cell the intensities at the 735 nm channel increase and then rapidly decrease. This effect is due to changes in the refractive index of the solutions in the cell. Although the leading edge of the slug caused undesirable intensity changes, the tail end of the slug mixed well with the ensuing pulses of water (Figure 3.9B). By observing the trailing end of the slug where indicator concentrations are lower than 1.00×10^{-5} M, pH measurements can then be collected.

A single freshwater measurement cycle is illustrated in Figure 3.10. In Figure 3.10A the absorbances (calculated from the raw intensity signals) exhibit a decline as the total indicator concentration (Figure 3.10C, the determination of the total indicator concentration will be addressed in a later section of this chapter) is diluted by the sample. By using the temperature that is collected during each measurement cycle, the molar absorptivity ratios (e's) and the pK_a' can be calculated using Table 3.1 and Equation 6 and Equation 9, respectively. Then by inserting the pK_a', molar absorptivity ratios, and the absorbances into Equation 5, a pH for each of the 14 intensity measurements can be determined. Figure 3.10 is a single indicator pulse from a river water sample, showing the 14 intensity measurements obtained during the 14 pulse sequence.

Figure 3.10B demonstrates the perturbation effect of the indicator on the pH of a freshwater sample. As the concentration of indicator decreases, the measured pH plateaus near the "true pH" (free of perturbation). The indicator perturbation will be discussed in more detail later.
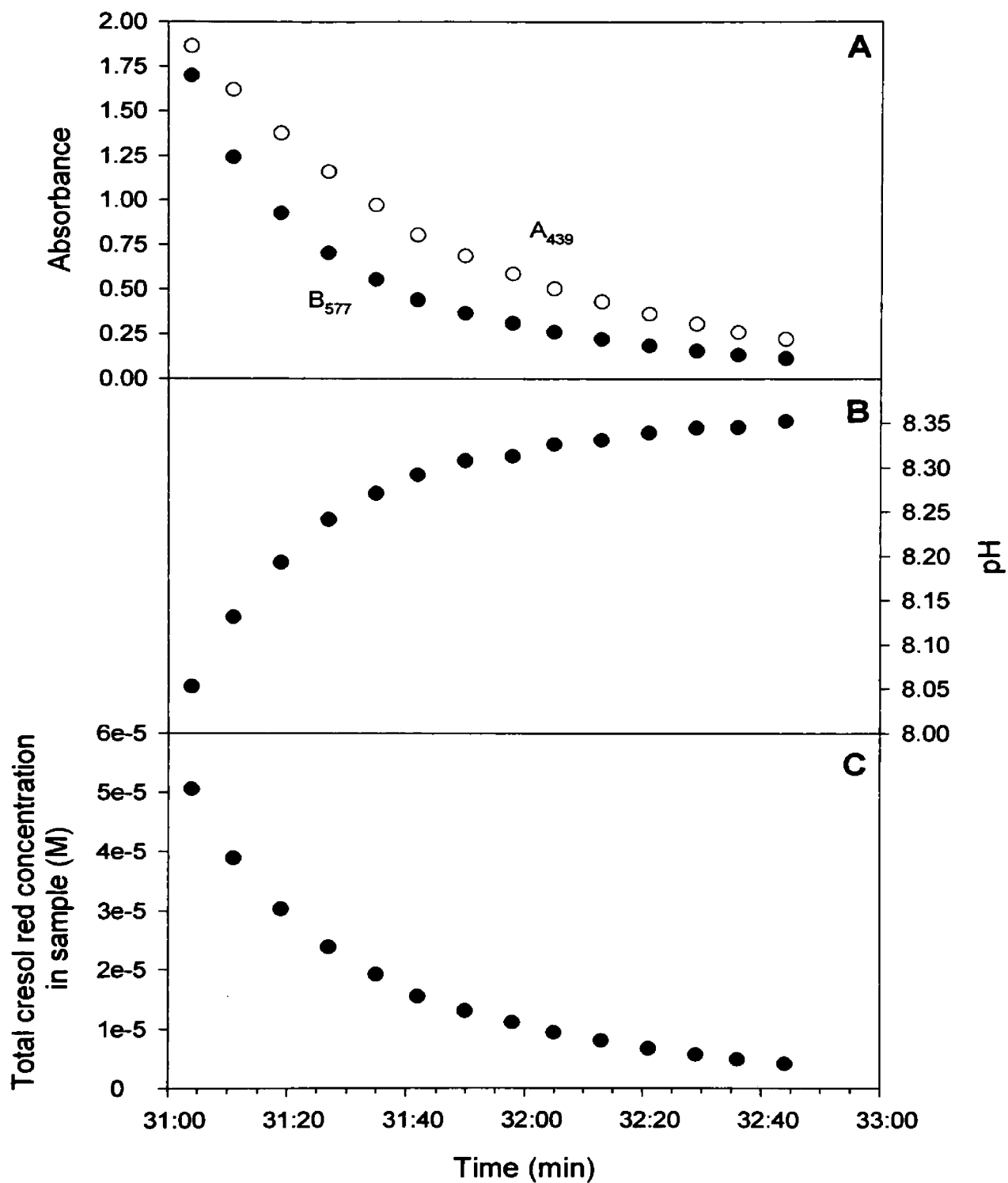
Figure 3.10. Data for a single indicator pulse from the December 1999 deployment, showing absorbances, pH, and indicator concentration for the 14 intensity measurements.

3.5 Power Draw and Deployment Duration

The power usage of the instrument components had to be assessed to determine the in situ duration of the instrument. Two separate power sources, a 16 C-cell 12-V internal battery pack (14,000 mA·hr) and an 18 D-cell 13-V external battery pack (30,000 mA·hr) (Figure 3.4), are utilized with the autonomous instrument. From Table 3.3 the data logger is displayed as having no current draw during the indicator and blank cycles, this is because it is continually powered. The 14,000 mA·hr supplies the needed power to the data logger. The other instrument components (pump, valve, light, and detector amplifier) are powered by the 30,000 mA·hr source.

Table 3.3. Current draws for the components of the SAMI-pH during blank and indicator measurement cycles.

Item	Current (mA)	Time On (sec) [For indicator cycle]	Time On (sec) [For blank cycle]	Current Draw (mA·hr) Indicator	Blank
Data Logger	20	Always On	Always On	NA	NA
Amplifier Detector	70	129	252	2.51	4.90
Valve	120	1	2	0.03	0.07
Pump	210	33	92	1.93	5.37
Light	120	121	212	4.03	7.07
			Total	8.60	17.05

For the 14,000 mA·hr power supply, the data logger has a continuous draw of 20 mA (Table 3.3), therefore its duration is 700 hrs (14,000 mA·hr/20 mA) or 29 days. With the 30,000 mA·hr power source the indicator and blank cycle mA·hr draws have to be converted into a daily usage. The daily power draw of the SAMI-pH's component can be calculated as follows:

$$\text{pH cycle} = \frac{2(8.60 \text{ mA} \cdot \text{hr})}{\text{hr}} \times 24 \text{ hr day}^{-1} = 413 \text{ mA} \cdot \text{hr} \cdot \text{day}^{-1}$$

$$\underline{\text{Blank cycle} = \hspace{6cm} = 17.05 \text{mA} \cdot \text{hr} \cdot \text{day}^{-1}}$$

$$\text{Total} = 430 \text{ mA} \cdot \text{hr} \cdot \text{day}^{-1}$$

In the calculation it is assumed that there would be a pH measurement twice every hour (2 x 8.60 mA·hr, from Table 3.2) and a blank once a day. The resulting duration of the 30,000 mA·hr source is then an addition of the daily power draw from the indicator cycle and a single blank cycle, which is ~69 days (30,000 mA·hr/430 mA·hr·day⁻¹). The data logger is the limiting factor for the in situ instrument, allowing it to last for approximately 1 month. The power restriction of the data logger can be dramatically improved by using other commercially available low power data loggers.

3.6 Precision and Relative Accuracy

Precision is very important for any instrument to be credible or usable. One way to check the precision of an instrument is to determine the agreement between measurements under constant conditions. The desired precision for the SAMI-pH is $\leq$

±0.010 pH units. To test the precision of the autonomous instrument, river water samples from the Clark Fork River near The University of Montana were collected in 500 ml glass bottles fitted with Teflon sealed caps. The bottles were acid washed and rinsed before collection to ensure they were free of contaminants. When collecting samples from the river, the bottles were rinsed three times with river water and then filled to the top and capped immediately leaving little or no headspace. The samples were then promptly transported back to the laboratory where the water was filtered to extract all the biota and particulates. The samples were then brought to atmospheric saturation, with respect to CO_2, to reduce chance of error that could occur due to gas exchange.

Once the water was equilibrated with atmospheric CO_2 (solution was stirred for ~2 hours) it was placed in an evacuated reagent (sample) bag via a syringe. This procedure was used to ensure that the reagent bag was free of air. The bag was then attached to the instrument for analysis.

A thermostated chamber, placed on the top of the instrument, was used to regulate the temperature. The chamber is designed to make a watertight fit around the top end cap of the SAMI-pH so that it could be filled with water to surround the external components (pump housing, flow cell, and the reagent and sample bags). A Bath/Circulator (Neslab, RTE 111) pumped water into a copper tubing heat exchanger within the chamber to maintain a constant temperature. The temperature was monitored using the SAMI-pH thermistor. Once the desired temperature was achieved, continuous sample measurements were taken. Results for the test are presented in the next chapter.

Relative accuracy is a term used to describe the accuracy of a measurement relative to another method. The relative accuracy of the SAMI-pH was determined with respect to measurements on an UV-VIS spectrophotometer. The relative accuracy between the two methods has previously been found to be ≤0.008 pH units (French 1999).

3.7 Determination of the Total Indicator Concentration

To characterize the perturbation of cresol red on a freshwater sample (presented in the next section), the total concentration of the indicator in the optical pathlength was determined. As Figure 3.2 shows the recorded absorbance signals at the 577 nm channel is strictly from the base form. From this observation, the concentration of the base form can be found by using Beer's Law,

$$[L^{2-}] = \frac{A_{577}}{\varepsilon_{577} b} \tag{19}$$

where b is the optical pathlength and A_{577} and ε_{577} are the absorbance and molar absorptivity at 577 nm respectively. From the Henderson-Hasselbalch equation (Equation 5) the concentration of the acid form can be determined as follows:

$$\frac{Base}{Acid} = \left(\frac{[L^{2-}]}{[HL^-]} \right) = \left(\frac{R - e_1}{e_2 - Re_3} \right) \tag{20}$$

and with rearrangement the acid form can be calculated by,

$$[HL^-] = \frac{[L^{2-}]}{\left(\dfrac{R-e_1}{e_2-Re_3}\right)}. \qquad (21)$$

Finally, the total indicator concentration could then be calculated with:

$$C_T = [HL^-] + [L^{2-}]. \qquad (22)$$

This technique allowed the pH perturbation dependence on C_T in both the SAMI-pH and the UV-VIS operations to be determined.

3.8 pH Perturbation

Dilution of the river sample by the indicator solution, effects of the indicator on different alkaline samples, and the addition of a weak acid indicator to a freshwater sample were determined.

Addition of the indicator can dilute the sample. However, because of the small dilution factor, dilution has a very minimal effect on the freshwater pH. The UV-VIS spectrophotometric method uses a 10 cm cell that has a 28 ml volume. To that volume 25 μL of cresol red is added resulting in a 0.09% dilution of water sample. In FRESHH2O.BAS the dilution factor results in a pH change of <0.0002 pH units.

Cresol red is a weak acid and when added to a poorly buffered sample it causes a decrease in the sample pH. The magnitude of the pH perturbation depends on the sample's acid neutralizing capacity. A theoretical program called PHINDICATOR.BAS, written in QuickBasic (Microsoft Corp.) by Mike DeGrandpre, was used to characterize

the effect of the indicator on various alkaline freshwater samples. The program utilizes carbonate alkalinity, temperature, indicator concentration, pK_a', and dissolved inorganic carbon (DIC) to determine the pH perturbation (ΔpH). Since PHINDICATOR.BAS program was not capable of computing the DIC, another program, FRESHH2O.BAS, was used to compute it. FRESHH2O.BAS is a freshwater version of the CO2SYS.BAS program (Lewis and Wallace 1998), converted by Matt Baehr, that calculates the carbonate parameters (DIC, alkalinity, pH, and pCO_2) if two or more of the parameters are measured or known.

For the conditions specified in Figure 3.11 caption, when the alkalinity is above 2250 μM there is a minimal change in the pH perturbation of a freshwater sample. Conversely, with alkalinities lower than ~2250 μM the indicator perturbation increases exponentially. The alkalinity range in the Clark Fork River varied from ~2500 μM to ~2900 μM during October 1998 to March of 1999 (Ronald et al. 1999, unpublished data). The difference in the perturbation over this range results in a difference of only 0.004 pH units.

In situ pH and indicator concentration can be used to determine the pH perturbation in lower alkalinity waters (< 2250 μM). A plot of pH against indicator concentration is nonlinear over the full range of indicator concentrations. But as the pH reaches indicator concentrations of 9.0×10^{-6} M and lower the plot becomes linear (Figure 3.12). From this observation an extrapolation back to the y-axis (pH) can be performed to find the unperturbed pH.
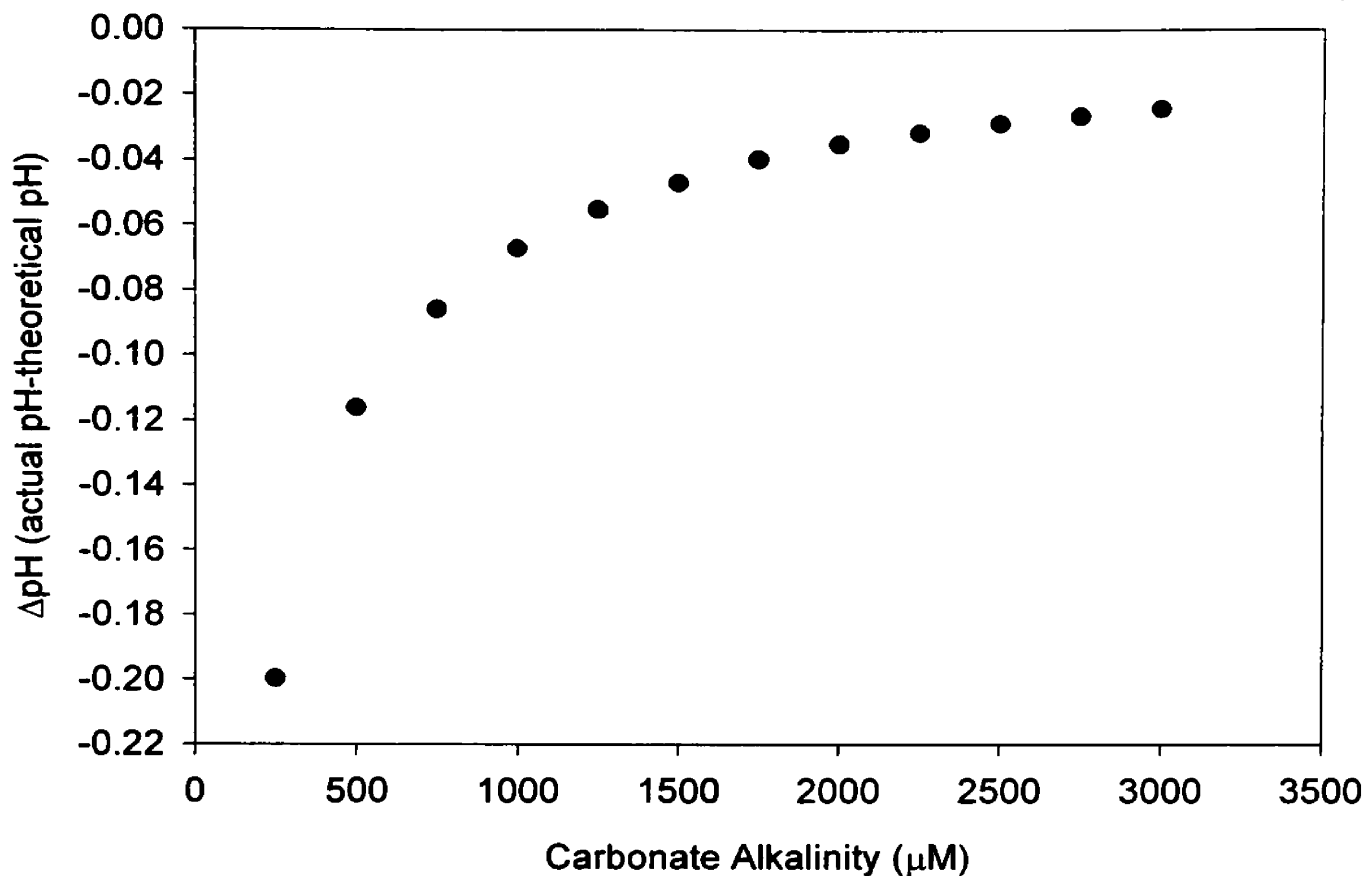
Figure 3.11. For small alkalinity changes above ~2250 μM there is little change in the pH perturbation. Whereas below 2250 μM concentrations there is a substantial change observed (minimum of ~0.01 pH units over a 500 μM change in alkalinity). The actual pH used was fixed at 8.4675 at a temperature of 10 °C and an indicator concentration of 6.00×10^{-6} M.

Rather than using multiple measurements as in Figure 3.12 to estimate the perturbation theoretical estimates can be obtained with an approximate sample alkalinity. Theoretical modeling of the pH perturbation was accomplished using the PHINDICATOR.BAS. Initially, an alkalinity of 2600 μM and a pH of 8.397 were used to compute a DIC at a temperature of 20°C. The resulting DIC and the alkalinity were used in the PHINDICATOR.BAS program over varying indicator concentrations to find the pH perturbation on a freshwater sample (Figure 3.13).
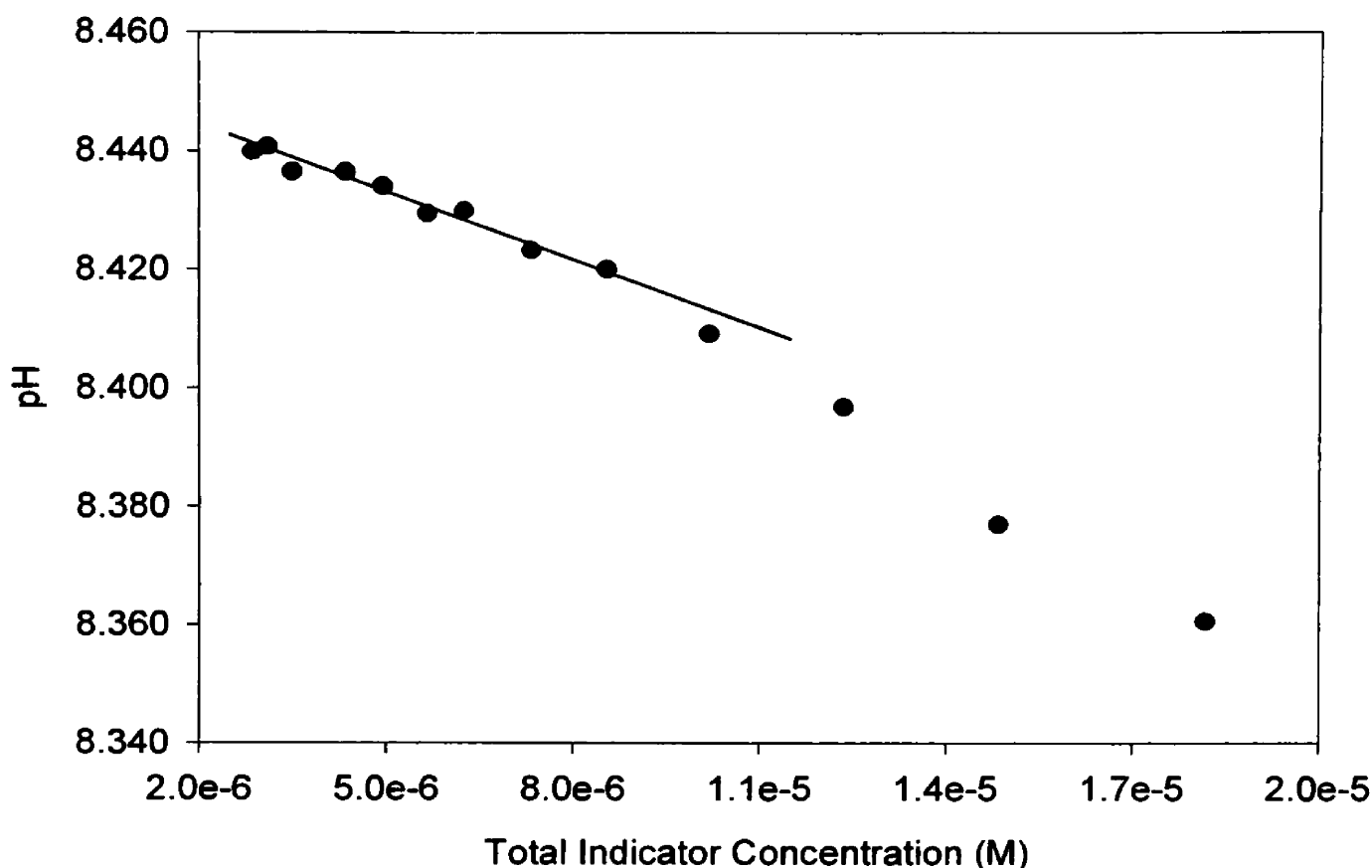
Figure 3.12. A single pH measurement of a freshwater sample measured by the SAMI-pH. The overall plot is non-linear in shape, but as the indicator concentration decreases below 9.0×10^{-6} M the curve can be assumed to be linear.

Experimental determination of the pH perturbation can be attained by adding small increments of cresol red indicator to river water sample and measuring on the UV-VIS. This experiment used a 10 cm jacketed cell that was thermostated at $20 \pm 0.1 °C$. Initially a blank, using river water, was obtained after the desired temperature was reached. To the blank 10 µL increments of indicator solution (1.008×10^{-3} mol kg^{-1}) was added until 2 a.u. was reached at the acid or base wavelength. The absorbances, which used to calculate the indicator concentration, were then plotted against the calculated pH (Figure 3.13). The data were linear over the range of indicator additions ($r^2 = 0.9570$).
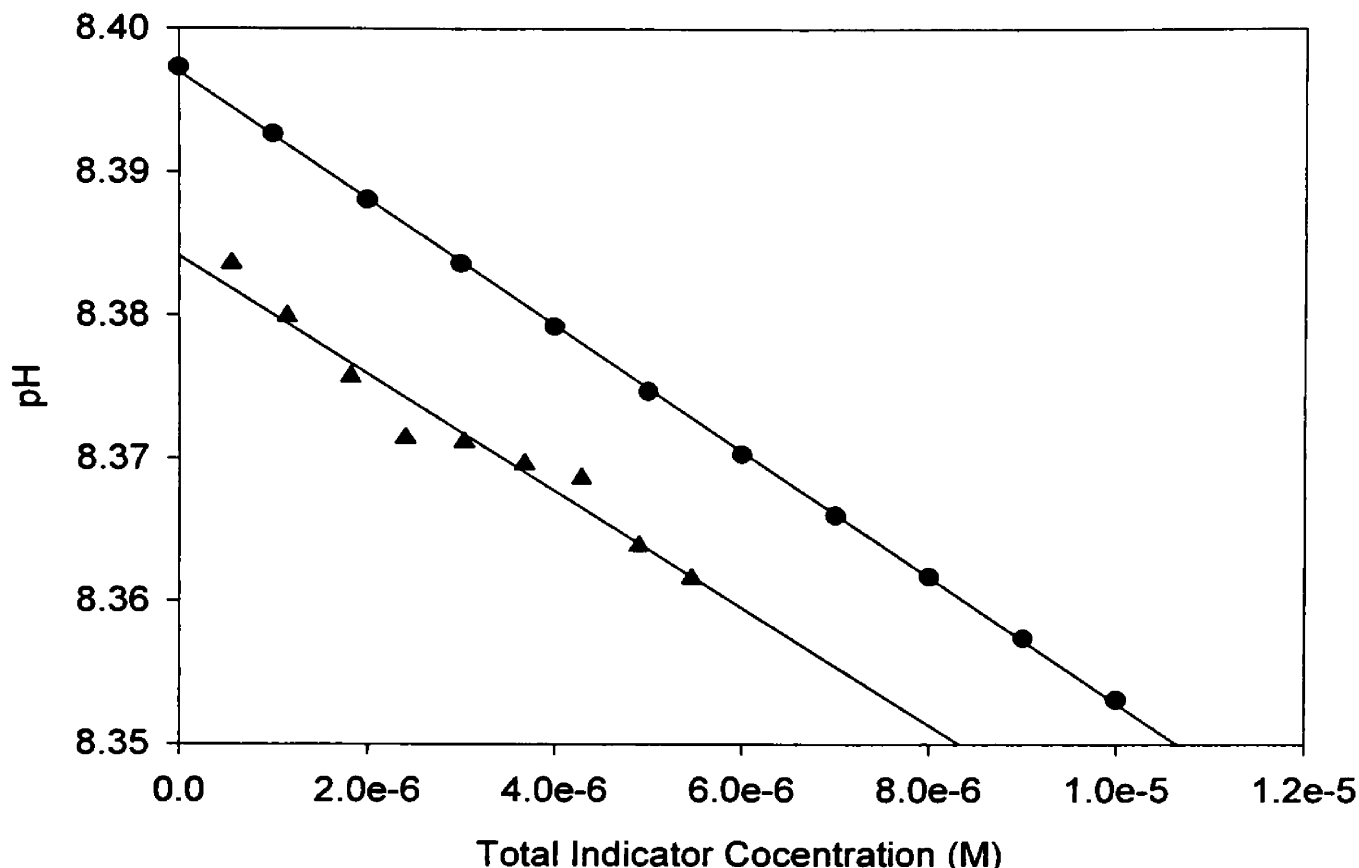
Figure 3.13. Theoretical perturbation (●) calculated using PHINDICATOR.BAS with an alkalinity of 2600 μM, a DIC of 2683 μM, and temperature at 20 °C . Experimental perturbation (▲) was performed using 10 μL increments of a 1.008×10^{-3} mole·kg^{-1} cresol red solution also at 20 °C. The linear regression output for the theoretical and experimental data resulted in slope of -4413 pH units M^{-1} and -4103 pH units M^{-1}and a r^2 of 0.9998 and 0.9570, respectively.

By virtue of the theoretical and experimental methods being linear, the pH perturbation for the two methods can be determined by using two different concentrations. To compare the UV-VIS and the SAMI-pH, indicator concentrations of 1.0×10^{-6} M for the UV-VIS and 6.0×10^{-6} M for the SMI-pH will be used to determine the pH perturbation. These concentrations are used because the resulting absorbances for each method are approximately equal at the 439 and 577 nm channels. The theoretical

and experimental methods resulted in slopes of -4413 pH units M^{-1} and -4103 pH units M^{-1}, respectively. The difference in the calculated pH perturbation between the two methods was in good agreement, 0.002 pH units (Table 3.4). Based on these tests, a pH for any given concentration can be determined using pH for a single indicator concentration and the slope from linear regression of the theoretical data.

The method just described can be implemented to obtain the unperturbed pH. For example, if the SAMI-pH found a water sample to have a pH of 8.465 at a concentration of 6.0×10^{-6} M the resulting pH at 0.0 M indicator would be calculated as follows,

$$pH_{unperturbed} = 8.465 - \left[(6.0 \times 10^{-6} M \times -4413) - (0.0 M \times -4413) \right] = 8.492$$

giving a pH perturbation of 0.026 pH units.

Table 3.4. The theoretical and experimental calculated pH the perturbation experiments are at indicator concentrations of 1.0×10^{-6} M and 6.0×10^{-6} M.

	1.0×10^{-6} M	6.0×10^{-6} M	Differences in the Calculated Perturbation
Theoretical pH	8.493	8.470	0.022
Experimental pH	8.380	8.356	0.020

3.9 Deployment of the Autonomous Instrument

3.9.a. Preparation of SAMI-pH for Deployment

Once the instrument was laboratory tested, the instrument was ready for deployment in the selected study site (the Clark Fork River). Before the instrument was deployed a few precautionary steps were taken to ensure that the instrument would not be damaged by debris in the river. First a protective copper cage was placed around the external components to keep the exposed fiber optics and tubing from being damaged. The instrument was then securely fastened into a stainless steel cage for added protection and to help anchor it on the river bottom (Figure 3.14). To secure the instrument on the riverbed, two cement anchors were attached to the stainless steel cage and placed upstream from the instrument.

3.9.b. Deployment Sites

The SAMI-pH was deployed in two different sections of the river on three separate occasions. One site is a short distance due east of The University of Montana, marked A in Figure 3.15. The other site is located east of East Missoula at the Sha-Ron fishing access located just north of the Bandmann Bridge, marked B in Figure 3.15. The second site was a preferred location because the water had a high flow rate to reduce biofouling and the site was also more accessible for discrete sample collection.

Figure 3.14. SAMI-pH in the protective cage, ready for deployment

3.9.c. Deployments of SAMI-pH and Other Instrumentation

This section will describe the three deployments and what improvements and tests were performed on the autonomous instrument to ready it for the next deployment. The first deployment was east of The University of Montana (marked A in Figure 3.15), the second and third deployments were near the Sha-Ron fishing access (marked B in Figure 3.15). The experiments will be described in the order they occurred. The results of the deployments will be presented in the next chapter in the same format as this section.
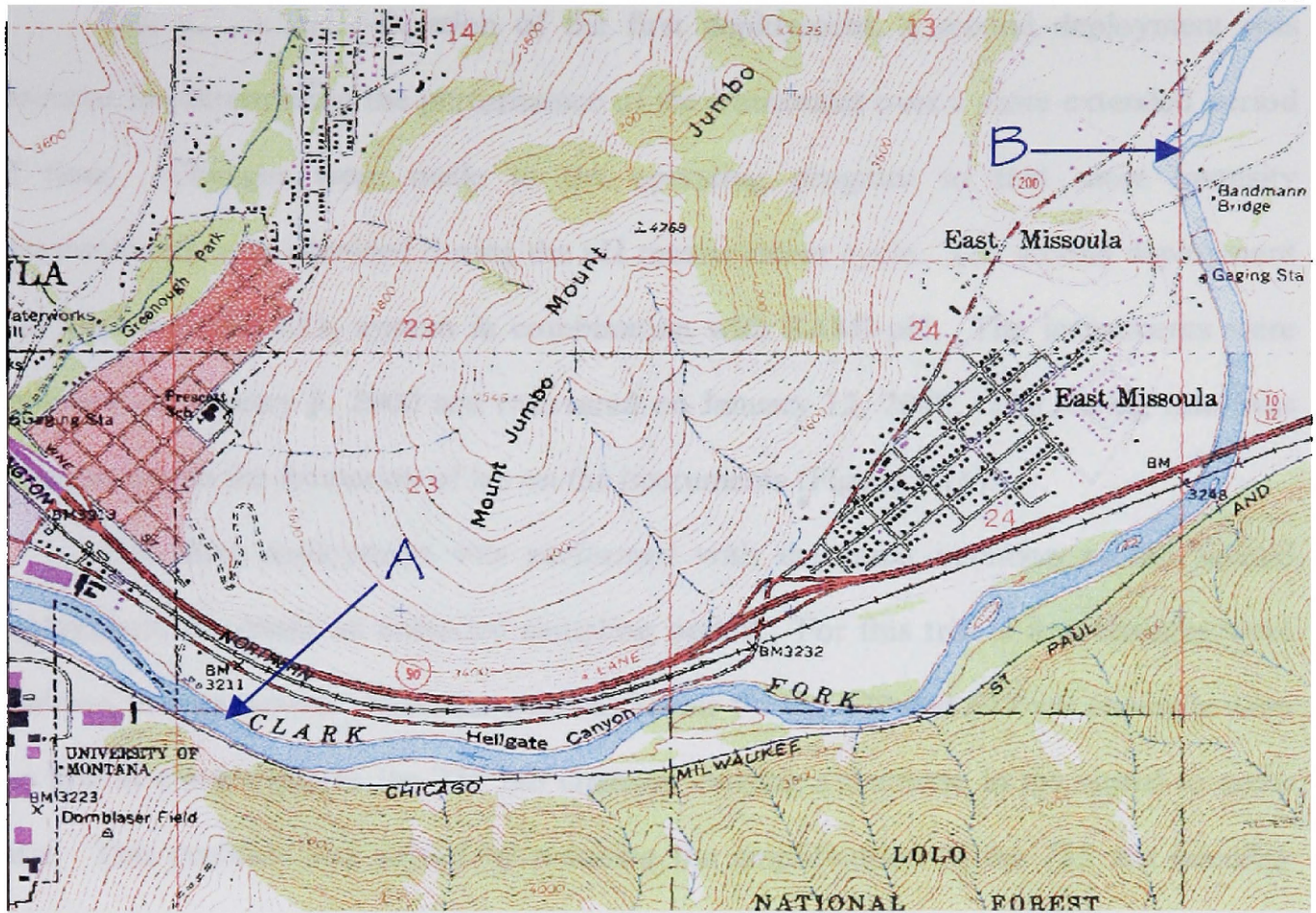
Figure 3.15. The SAMI-pH was deployed in the Clark Fork River near Missoula, MT at two different sites, one just east of The University of Montana (A) and another north of the Bandmann Bridge east of East Missoula, MT (B).

The SAMI-pH was first deployed on December 22, 1999 and retrieved on December 24, 1999. The instrument was programmed to collect pH data every 15 minutes. During the experiment Jason Reynolds had deployed an autonomous sensor that monitored the partial pressure of CO_2 (pCO_2), SAMI-CO_2 (DeGrandpre et al 1997), at same site as the SAMI-pH. The advantage of having additional instrumentation is that it enables independent calculations of pH for comparison with the SAMI-pH performance.

Due to the short duration of the first deployment, a second deployment was essential for determining the performance of the instrument over a more extended period of time. Changes were made to the operating program so that more intensity measurements were obtained during the pH measurement cycle. The second deployment also used a SAMI-CO_2 system in combination with SAMI-pH. The instruments were deployed on January 8, 2000 and recovered on January 12, 2000. The testing time was cut short due to the formation of ice on the instruments (Figure 3.16).

The third deployment was performed with the same intention as the second deployment, to obtain an extended sampling period. For this trial a few changes were made on the instrument. First, the intensity levels for the 439 and 577 nm channels were too low in comparison to the 735 nm channel, causing a decrease in the signal-to-noise ratio. This problem was solved by reducing the amplification of the 735 nm intensity signal (reduction in the feedback resistance of the 735 nm channel) and increasing the light intensity through the optical system (moved the fiber optic closer to the light source). The operational program was changed so that 10 pulses of water would precede the original indicator and water sample pulses. This change was made to account for the dead volume in the pump and valve, as well as lag time between the inlet tubing to the valve. Additional samples were also collected for the analysis of alkalinity. Alkalinity was determined via potentiometric titration and subsequent Gran Plot analysis. The instrument was placed back in the river on October 29, 2000 and was recovered on November 3, 2000.
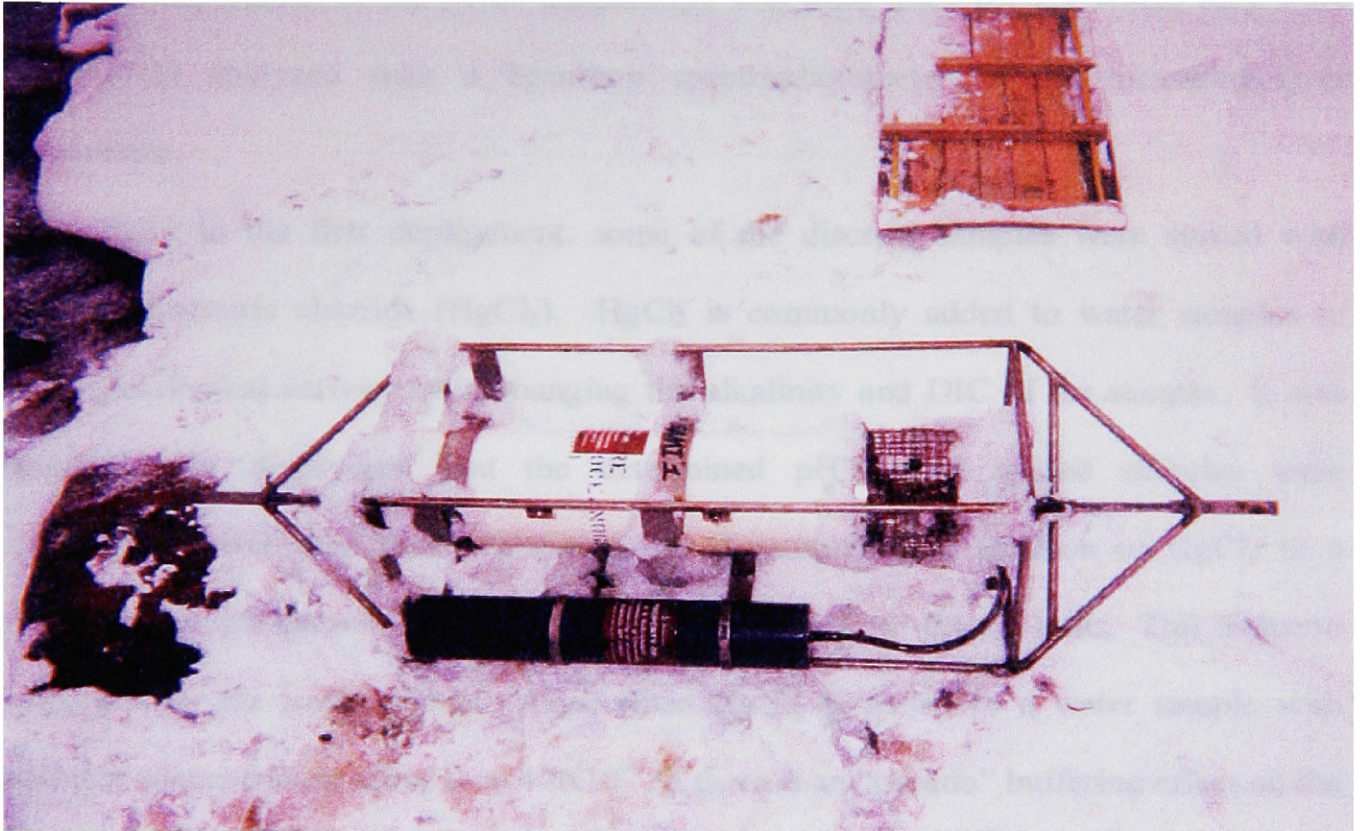
Figure 3.16. The deployment during January of 2000 was cut short due to the formation of ice on the SAMI-pH.

3.10 Discrete Sampling

Sampling was used to verify SAMI-pH measurements during each deployment. Discrete samples were obtained two to four times every day during the deployments. The bottles and sampling technique used are the same as discussed in section 3.6.a (excluding filtration and equilibration to atmospheric CO_2). After all the samples were collected the temperature of the river was obtained using a portable electronic temperature probe (Omega HHD, with a reported accuracy of ±0.1°C). The samples were transported back

to the lab in a bucket of ice (river temperature was from 6.0 - 0.1°C), where they were immediately analyzed with a benchtop spectrophotometer at the measured river temperature.

Prior to the first deployment, some of the discrete samples were spiked with saturated mercuric chloride ($HgCl_2$). $HgCl_2$ is commonly added to water samples to prevent biological activity from changing the alkalinity and DIC of the sample. It was serendipitously discovered that the determined pH's from spiked samples were consistently lower than that of the non-spiked samples. The addition of $HgCl_2$ to a freshwater sample causes an observed decrease in the pH of ~0.1 pH units. This is due to hydrolysis by the mercury ion. Also, when $HgCl_2$ is added to a water sample with indicator concentration lower than 4.0×10^{-6} M there is an "pseudo" buffering effect on the pH (Figure 3.17). For indicator concentrations larger than 4.0×10^{-6} M, there seems to be no deviation between the spike (with $HgCl_2$) and non-spiked samples. Although it is not concretely known on what causes this phenomenon, it is assumed that there is a complexation between the Hg^{2+} metal and the indicator, thereby causing an alteration in the pH perturbation. As a result, the discrete samples for the deployments were analyzed without the addition of $HgCl_2$. To limit the biological activity the discrete samples were transported immediately back to the lab for analysis (within 1 ½ hrs from the sampling time).

Discrete samples from the first and second deployments were analyzed in the lab with an UV-VIS spectrophotometer (Perkin-Elmer, Lambda 11). Portions of the freshwater samples were transferred into a 10-cm thermostated flow cell (that was rinsed three times with sample water) to which 75 µL of a 3.75×10^{-6} µmole kg^{-1} cresol red
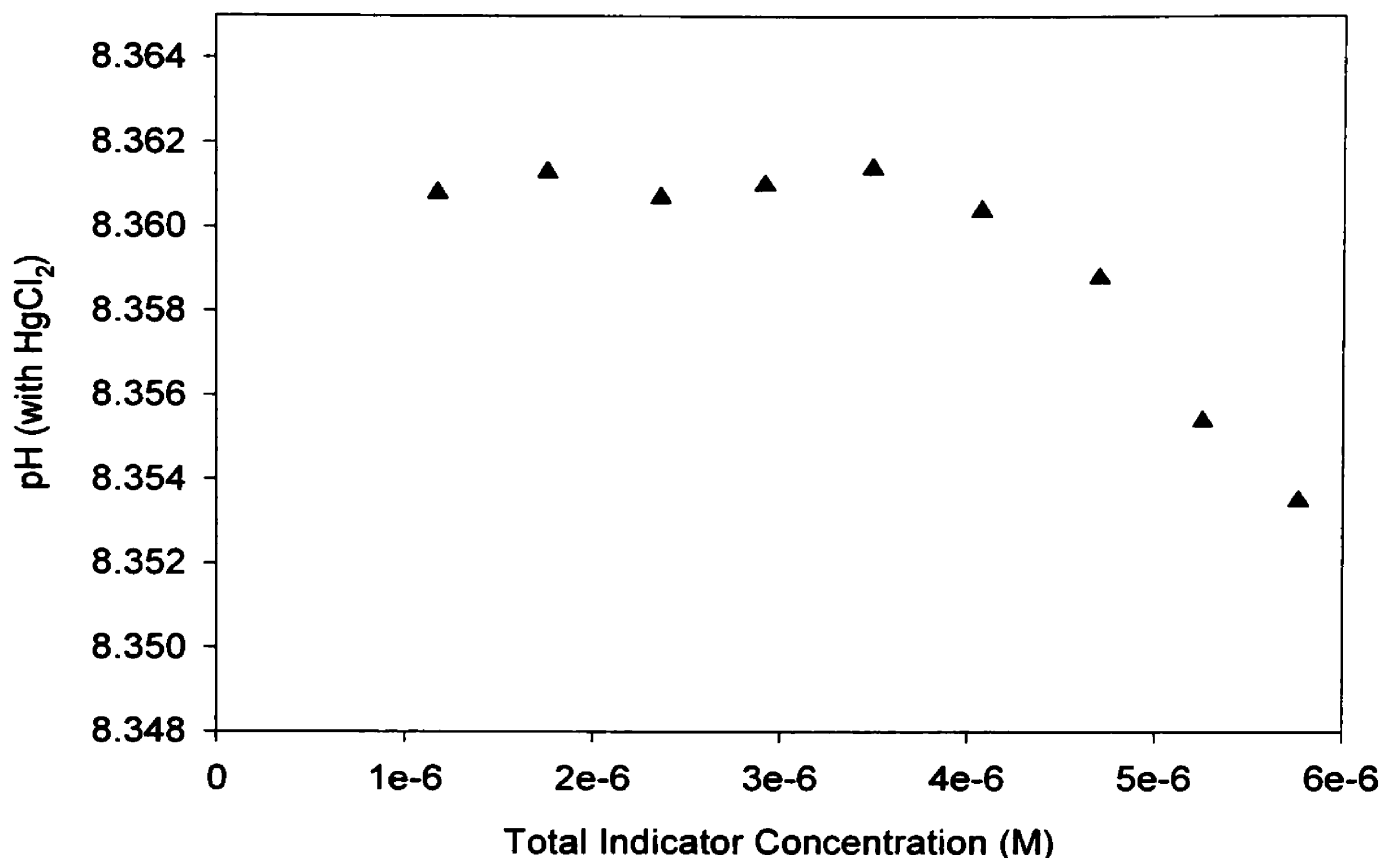
Figure 3.17. The addition of mercuric chloride to a freshwater sample causes an alteration in the pH perturbation at indicator concentrations below $4.0^{-6} \times 10$ M. This alteration is believed to be caused by complexation of Hg^{2+} with the indicator.

solution was added. The absorbances at 439, 577, and 735 nm were then collected. The analysis was performed three times for each discrete sample collected.

For the third deployment an UV-VIS spectrophotometer (Varian, Cary 300 Bio) was used for analyzing the grab samples. The Cary UV-VIS is a double beam spectrophotometer equipped with 10 cm cell holders that are temperature controlled using the bath/circulator (Neslab, RTE 111). A 10 cm cell filled with DI water is used as the

reference sample. Another 10 cm cell, filled with sample water, was placed in the sample beam where a blank was recorded. Then 25 μl of a 2.00×10^{-3} mole kg^{-1} of cresol red solution was added to the sample cell. The cell was then placed in the bath/circulator for 5 minutes to reach the desired measurement temperature. After the allotted time, the cell was set back in the UV-VIS to collect absorbance measurements.

3.11 Temperature Correction

The river temperature was measured by the SAMI-pH and by the previously mentioned portable electronic thermistor when discrete samples were collected. When the deployments were finished and the data were collected, the two temperatures did not always agree. Using the FRESHH2O.BAS program along with an alkalinity of 2780 μM, DIC of 2783 μM, and varying temperatures, the pH sensitivity to temperature was determined (Figure 3.18). From the resulting data, a linear offset was calculated and used to correct the UV-VIS data to the in situ temperature.

Experimental tests were also performed to characterize the effects of temperature on the pH of a river water sample. Two trials were done on the same discrete sample taken from the Clark Fork River. The tests utilized the same methods in the determination of the discrete samples during third deployment. The only exception was that the cell was placed back in the water bath where it was allowed to equilibrate to the next temperature.
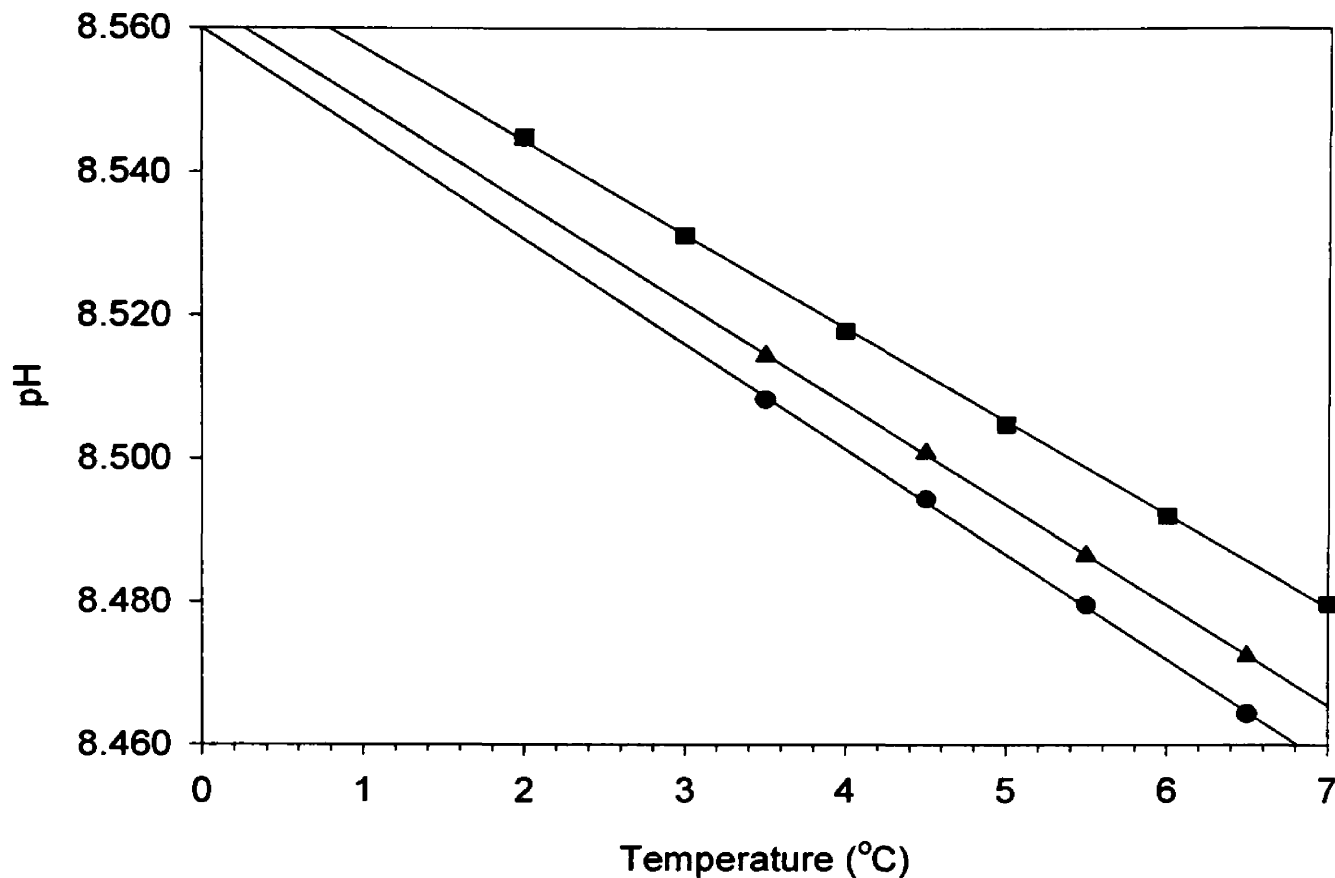
Figure 3.18. Theoretical (■) determination of freshwater pH variability with respect to temperature using an alkalinity of 2780 μM and DIC of 2783 μM. Linear regression resulted in a slope of -0.0127 pH units °C $^{-1}$, a y-intercept of 8.3309, and a r^2 of .998. The experimental determination of pH dependence on temperature was performed on a freshwater sample. The two experimental trials were performed using the same collection of discrete samples. The slope and correlation coefficient for the first trial (▲) are -0.0140 pH units °C $^{-1}$ and 0.9999 and for the second trail (●) are -0.0147 pH units °C $^{-1}$ and 0.9995.

The resulting slopes from the theoretical (-0.0127 pH units °C^{-1}) and experimental data (-0.0140 pH units °C^{-1} and −0.0147 pH units °C^{-1}) are within approximate agreement, resulting in a difference of ~0.002 pH units over a 1.00 °C temperature difference. Therefore the theoretical estimate can be applied for correcting the temperature difference between the SAMI-pH and the UV-VIS.

Chapter 4

Results

This chapter will present a comparison of data collected from the SAMI-pH and discrete samples during the three deployments. Changes made in methodology, data manipulation, or to the SAMI-pH will be presented in the order as they occurred during the research period. This format will provide a logical timeline for the changes that were made for the subsequent deployments. (All pH data in this section is uncorrected until corrections are discussed).

4.1. First Deployment

The data collected from the first deployment was imported into a Quattro Pro (Corel Corp.) file where the intensities were converted into absorbances (Equation 7) and ultimately into pH and blank values (Equations 5 and 14). Temperature, 735 nm intensity (I_{735}), absorbances (439 and 577 nm), and pH from the SAMI-pH were plotted versus year day for the full deployment (Figure 4.1). Temperature and calculated pH from the discrete sample analyses were also graphed with the in situ data.

Temperatures recorded during the grab samples were not in agreement with the in situ temperature (Figure 4.1A) with differences ranging from 0.5 °C to 0.1 °C. Therefore, temperatures from the CO_2 sensor were also plotted to determine which data set was valid. The temperatures from the CO_2 sensor were in good agreement with the SAMI-pH (better than 0.1 °C) over the duration of the deployment. The temperature difference between the SAMI-pH and UV-VIS will be addressed throughout this chapter.
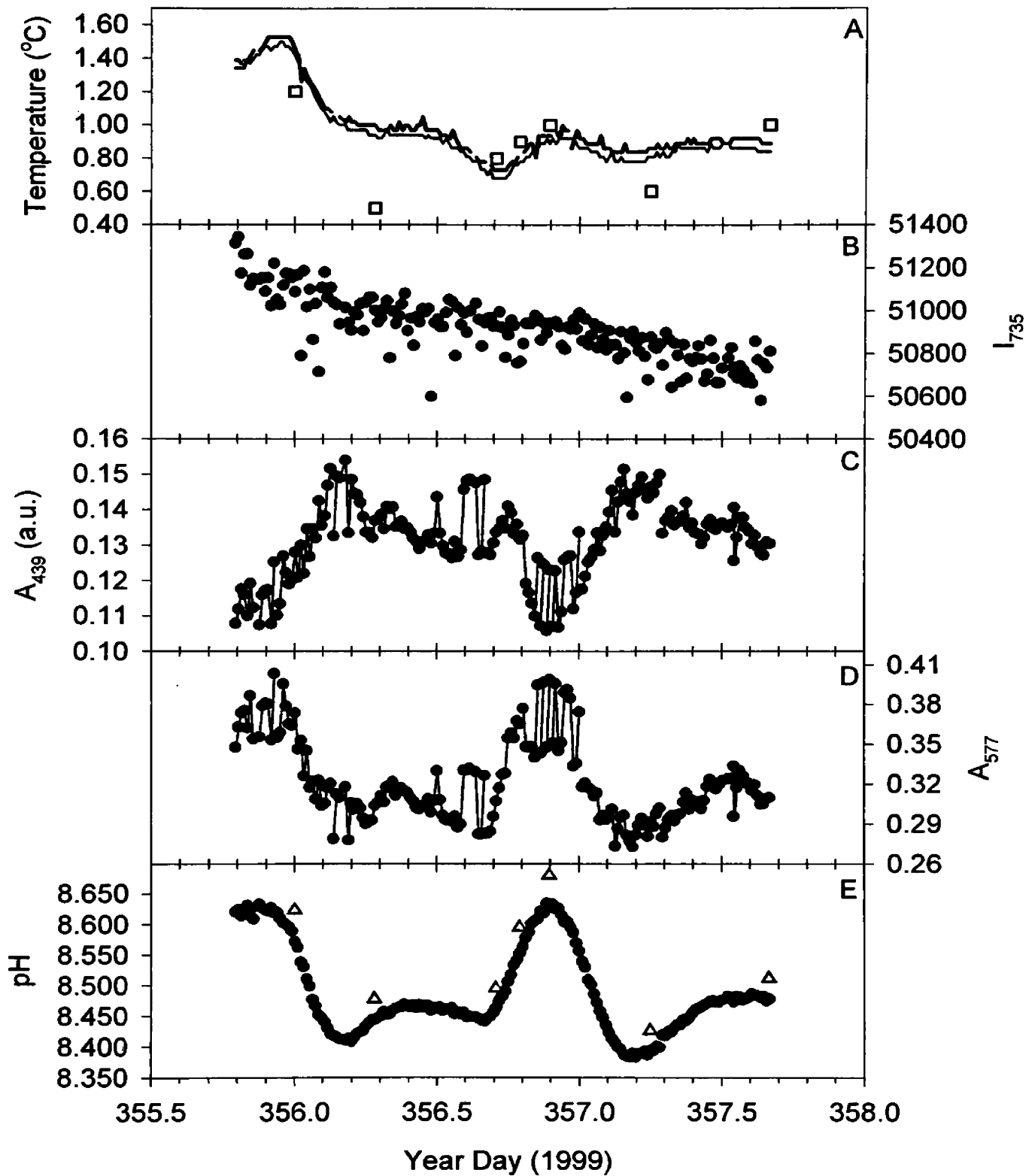
Figure 4.1. Data collected from the SAMI-pH during the December 1999 deployment (in black). Along with temperature (□) and pH data (△) from the discrete samples and temperature from the SAMI-CO₂ sensor (-).

The plot of the reference wavelength intensity (I_{735}) versus year day demonstrates its slight dependence on temperature (Figure 4.1B), as the temperature decreases the resulting output intensity decreases. This effect is probably due to changes in the light throughput through the flow cell due to contraction and expansion of the cell. This illustrates why it is important to correct for the intensity fluctuations using a reference channel during absorbance measurements.

According to the equilibrium expression (Equation 1), absorbances for the two forms of the indicator will be inversely related, it can be assumed that the two forms will act as "mirror images". For example, if the pH of a water/indicator solution was increased, then the acid form would be depleted causing a decrease in absorbance (Figures 4.1C). Conversely, the base concentration would increase, causing an increase in absorbance ($\propto\varepsilon$) (Figure 4.1D). This characteristic is useful in determining if the instrument was functioning properly. The step-like appearance in absorbance data is due to changes in indicator concentration. By calculating absorbance ratios, the fluctuation in the absorbance for the acid and base channel are canceled as seen in the pH data (Figure 4.1E). The average relative accuracy between the discrete sample calculations and the in situ measurements (UV-VIS - SAMI-pH) is 0.038 ±0.010 pH units (N = 7).

A diurnal cycle, with two maxima and a variability of about 0.250 pH units is observed when the pH from the SAMI-pH is plotted against the year day (Figure 4.1E). Freshwater pH is predominately controlled by the carbonate system and the processes that affect it, particularly the biological respiration and photosynthesis and also diffusion of CO_2 across the air-water boundary. By using the SAMI-CO_2 in combination with the SAMI-pH, the dependence of pH on the carbonate system can be characterized.
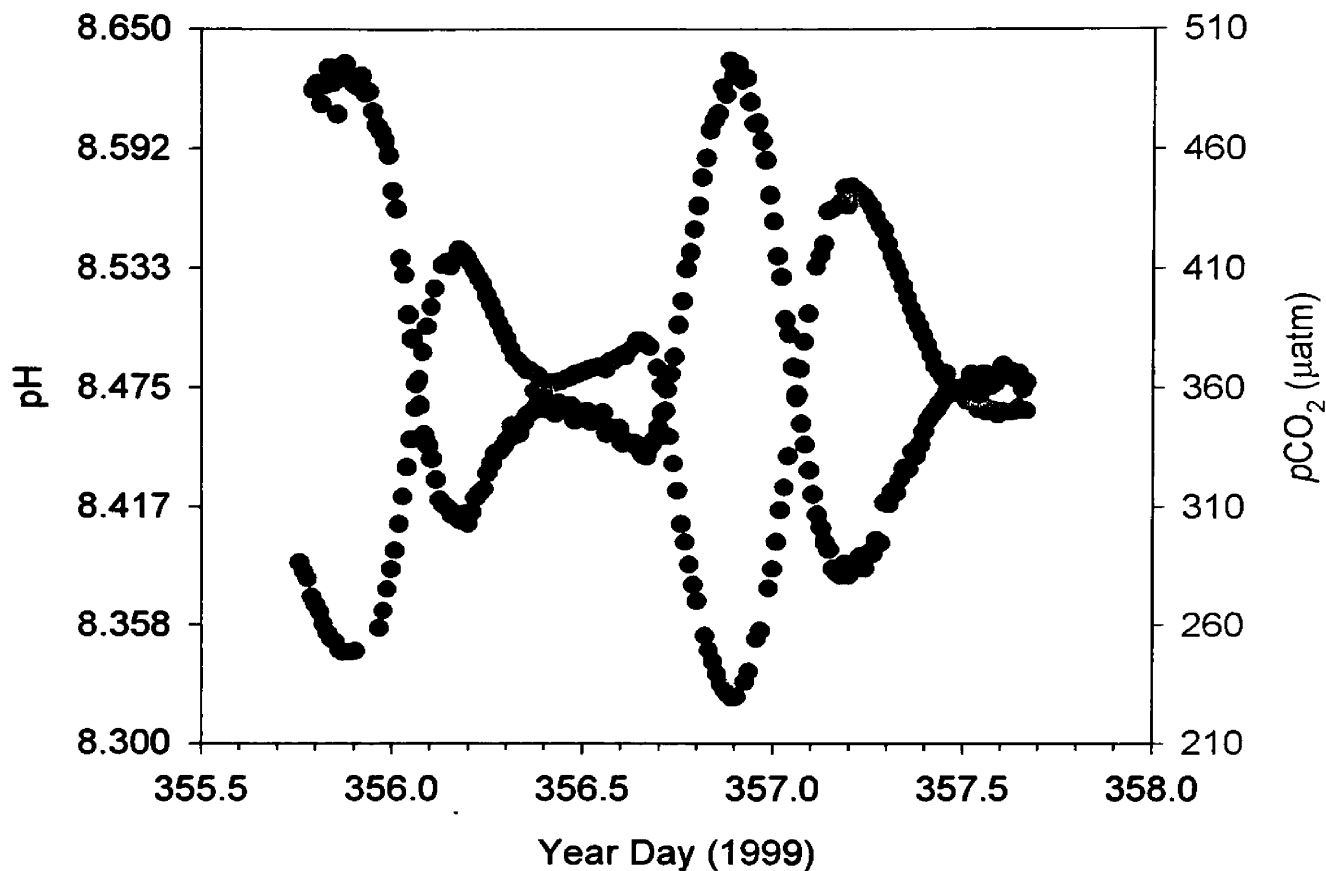
Figure 4.2. The pH (measured with the SAMI-pH) of the Clark Fork River appears to be predominately controlled by the partial pressure of CO_2 (pCO_2) (measured with the SAMI-CO_2).

Figure 4.2 illustrates the expected inverse relationship of pH with river pCO_2. Another advantage of monitoring the pCO_2 is that it can be used with another carbonate parameter (alkalinity or DIC) to calculate pH. Jason Reynolds collected periodic discrete samples for one week prior to the first deployment for the analysis of alkalinities. These data were used in conjunction with the pCO_2 to obtain a calculated pH (Figure 4.3). The calculated pH was on average ~0.1 pH units greater than the recorded in situ pH from the SAMI-pH. This plot will be discussed in the next chapter.
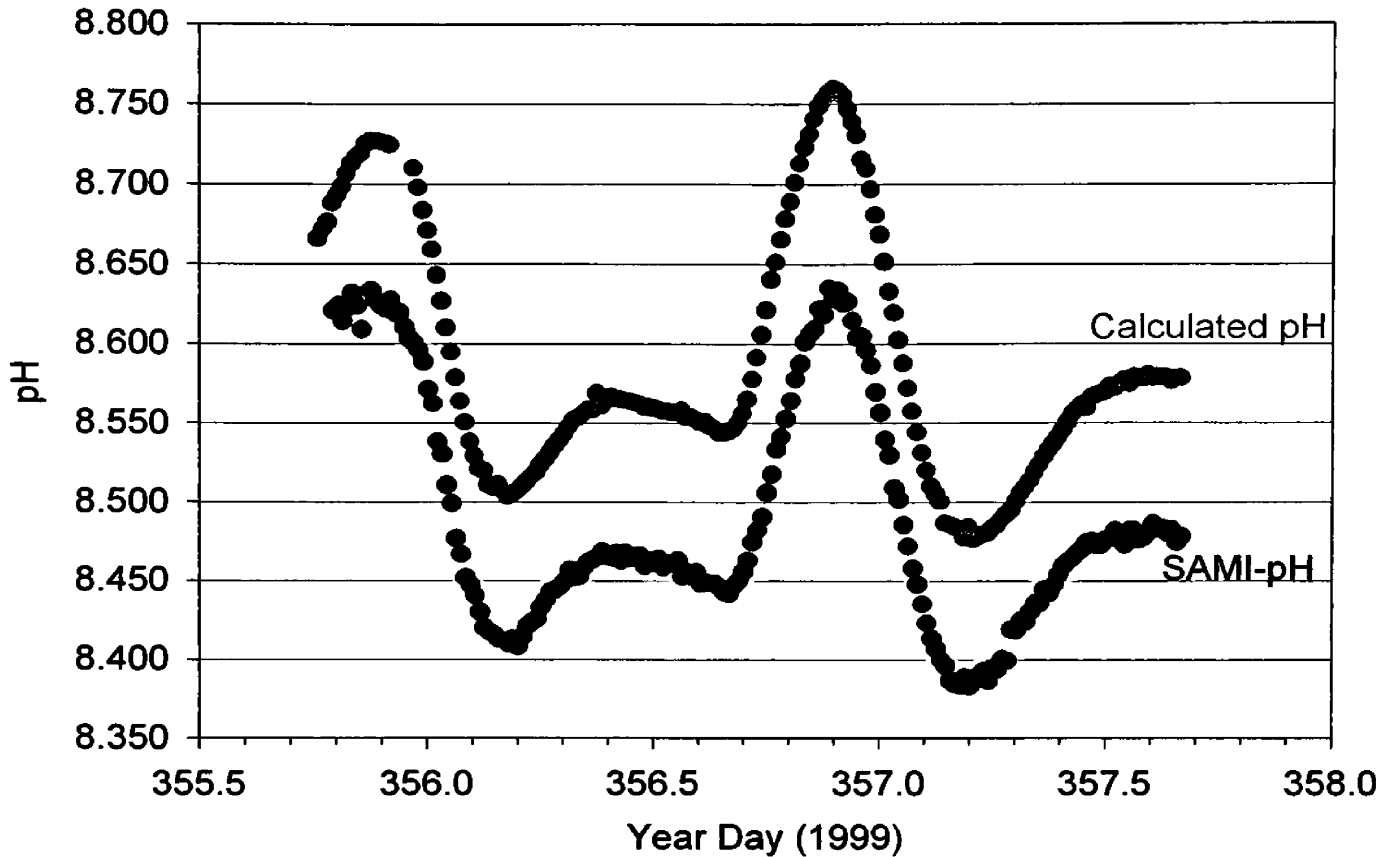
Figure 4.3. The calculated pH was determined using an average alkalinity of 2753 μM and the in situ pCO_2 and temperature data.

4.2 Second Deployment

A second deployment quickly materialized to collect data over a longer duration of about 7 days. The longer deployment would test the instrument's long-term stability and would also determine if the offset in the relative accuracy was reproducible. The only modifications made to the SAMI-pH were a recalibration of the spectrograph wavelengths and the number of intensities collected for the pH measurements cycle was increased from 14 to 18. A SAMI-CO_2 was again deployed adjacent to the SAMI-pH.

The second deployment, near the Sha-Ron fishing access east of East Missoula, included some mistakes and a little misfortune. As was stated in the previous chapter the

deployment was stopped short (only ~ 4 ½ days) due to instrument acting as a nucleation site for ice in the river. After the data from the SAMI-pH was downloaded, there was an error found in the operational program of the instrument. The instrument was programmed to collect data once every hour instead of 4 times per hour. This mistake led to few comparisons between the SAMI-pH and the calculated sample analyses. Also during the testing period, grab samples were not collected for alkalinity determination, therefore comparison between the SAMI-pH data and tabulated pH from pCO_2 and alkalinity could not be performed. The SAMI-pH functioned very well however, despite operator blunder.

The temperatures recorded during the grab sampling and by the SAMI-pH did not agree during the second river trial period. There was an observed differences greater than 0.25 °C (Figure 4.4A). The reference channel demonstrated the same dependence on temperature as the first deployment (Figure 4.4B). The pH data from the SAMI-pH demonstrated the same diurnal variability as in the first deployment, with two maxima per day and a variability of ~0.175 pH units. The graph of in situ and discrete sample pH versus year day (Figure 4.4C) exhibits a larger difference between the two methods than the first deployment. The relative accuracy between the two methods was approximately 0.067 ±0.013 pH units (N = 4).
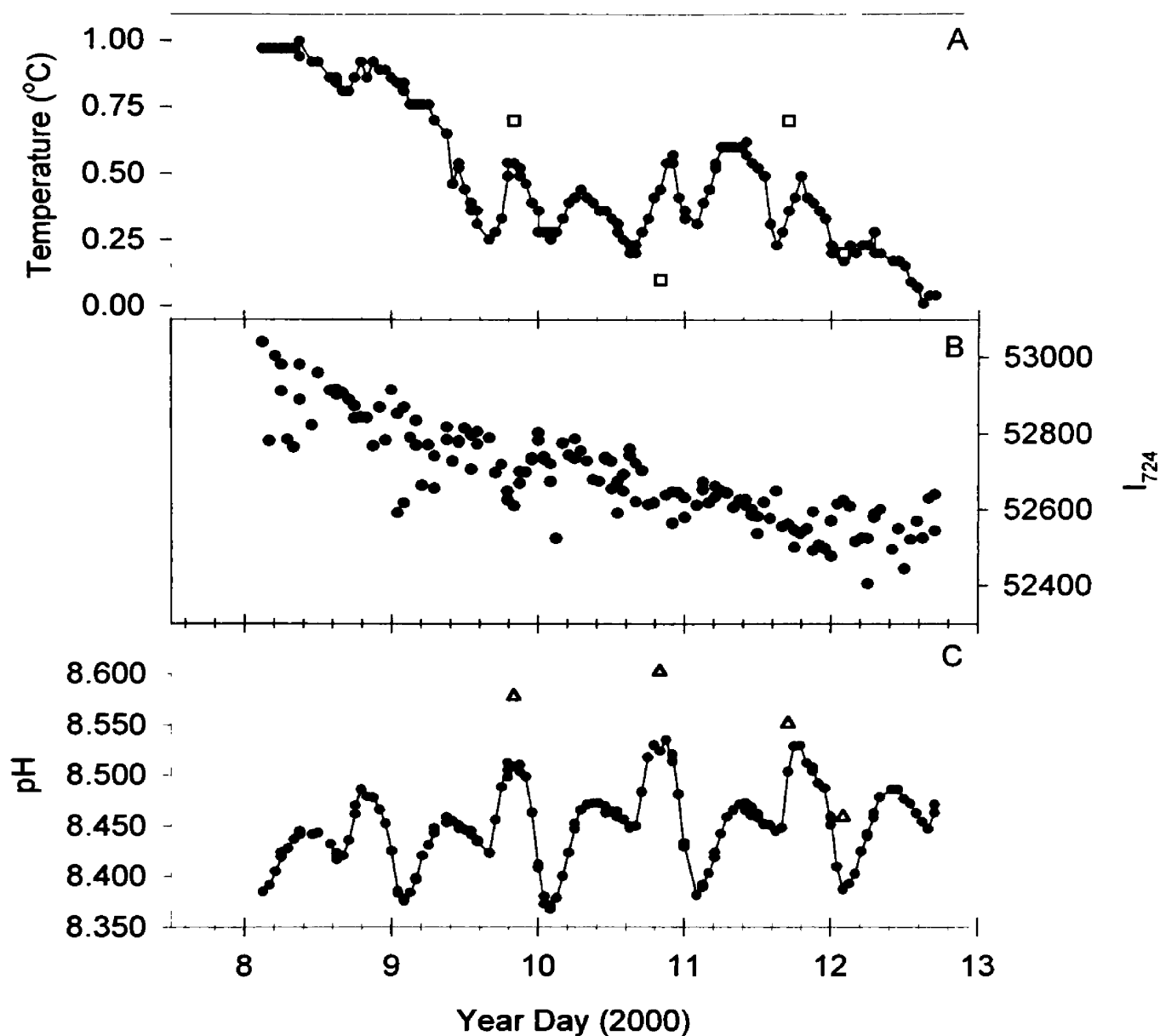
Figure 4.4. Data from the SAMI-pH along with temperature (□) and pH (△) from the discrete samples collected during the second deployment.

The pCO$_2$ and pH were plotted against year day to determine if the decrease magnitude in the diurnal cycle was real and also if the pH instrument was performing properly (Figure 4.5). The characteristic inverse relationship between the two carbonate parameters was very evident as was observed in the first deployment.
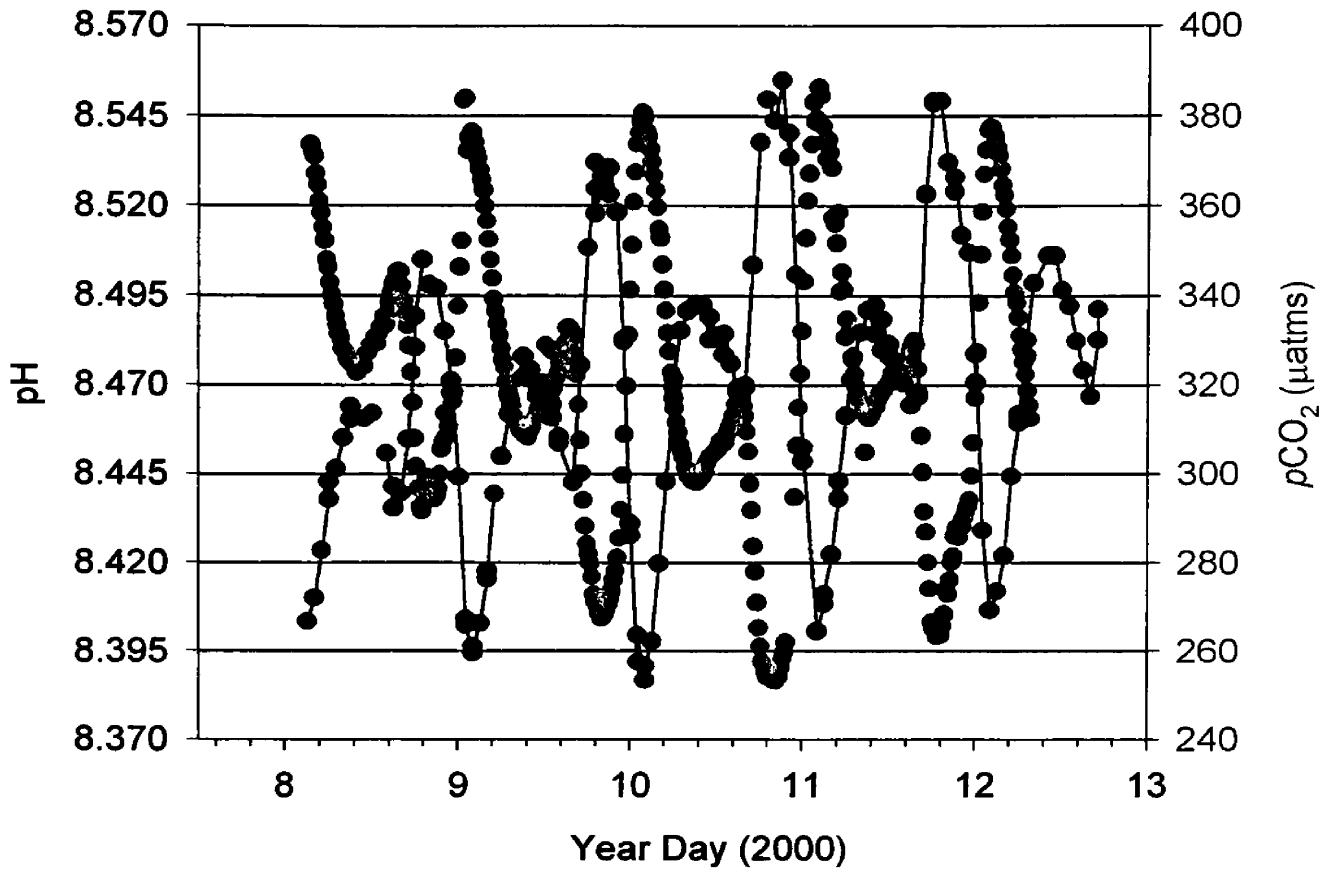
Figure 4.5. The characteristic inverse relationship between $p\text{CO}_2$ and pH was evident again during the second deployment. There was a decrease in the magnitudes of variability for both the $p\text{CO}_2$ and pH in comparison with the first deployment.

4.3. Experimental and Theoretical Corrections and Offsets

Before the SAMI-pH could be placed back into the river for a third time, the large difference in relative accuracy (within a deployment and between the two deployments) had to be addressed. As mentioned earlier, a relative accuracy of ±0.01 pH units is desired. Another issue investigated was the inconsistency in the temperatures of the external temperature probe and the thermistor of the autonomous instrument. Finally, modifications that were performed on the SAMI-pH to improve its performance will be addressed.

The first correction examined for improving the relative accuracy was the molar absorptivity dependence on temperature. We also discovered that the method of calculating the molar absorptivities over ±12 nm bandpass of the SAMI-pH was another source of error. Initially the molar absorptivities were computed by averaging absorbance over the ±12 nm range whereas the SAMI-pH averages intensities over a ±12 nm range. The problem with this method is that the absorbance is linear function and intensity is a nonlinear function with respect to the molar absorptivities. To resolve the problem, absorbances from the molar absorptivity experiments were converted into intensities, averaged, and then converted back into an absorbance.

Perturbation of freshwater pH by the addition of the cresol red indicator was also causing differences in the two methods. The pH perturbation was characterized theoretically and experimentally over a range of indicator concentrations so that an offset could be applied to the pH measurements.

With theoretical modeling, a correction for the dependence of freshwater pH on temperature was determined and applied to all discrete samples. After various experiments in the lab, it was concluded that the external temperature probe and the SAMI-pH work properly and were within ±0.2 °C of each other.

Once all of the corrections were determined, they could be applied to the first two deployments data sets to reassess the relative accuracy (Table 4.1 and 4.2). The molar absorptivity and pH perturbation corrections were applied to the SAMI-pH measurements. The molar absorptivity correction resulted in a pH increase of 0.019 pH units and the pH perturbation led to a range of corrections difference (ranging from −0.021 to −0.019 pH units) depending on the difference in indicator concentration

between the UV-VIS and SAMI-pH. The UV-VIS pH calculations were corrected by deducting the error associated with temperature (from −0.007 to +0.005 pH units).

With all of the corrections applied, the relative accuracy for the two deployments was improved but the discrepancy between the deployments was not (Tables 4.1 and 4.2). The average relative accuracy for the deployments was determined by calculating the mean offset and the standard deviation about the mean offset for the pH differences of all the trials. The corrected discrete samples and in situ data for the December 1999 trial

Table 4.1. The relative accuracy for corrected pHs for the SAMI-pH and discrete samples collected during the December 1999 deployment. (The mean offset is considered the average relative accuracy).

		SAMI-pH		UV-VIS	Δ pH (UV-VIS-SAMI-pH)
		Uncorrected	Corrected		
Year Day (1999)	356.00	8.5712	8.6105	8.6201	0.0095
	356.28	8.4441	8.4817	8.4708	-0.0110
	356.71	8.4630	8.5014	8.4959	-0.0055
	356.79	8.5526	8.5928	8.5966	0.0038
	356.90	8.6278	8.6684	8.6814	0.0130
	357.25	8.3941	8.4322	8.4223	-0.0100
	357.67	8.4782	8.5158	8.5133	-0.0025
				Mean offset	-0.0004
				Std. of mean offset	±0.009

Table 4.2. The relative accuracy for uncorrected and corrected pHs for the SAMI-pH and discrete samples collected during the January 2000 deployment.

		SAMI-pH		UV-VIS	Δ pH
		Uncorrected	Corrected		(UV-VIS-SAMI-pH)
Year Day	9.83	8.5087	8.5467	8.5806	0.0338
	10.83	8.5240	8.5632	8.5982	0.0350
	11.71	8.5036	8.5424	8.5560	0.0137
	12.08	8.3871	8.4267	8.4593	0.0326
				Mean offset	+0.0288
				Std. of mean offset	±0.0101

resulted in a mean offset of -0.004 pH units and a standard deviation of ±0.0004 pH units (Table 4.1). The January 2000 corrected data produced a mean offset of ±0.029 pH units (Table 4.2) and a standard deviation of ±0.010 pH units.

With all of the modifications to the SAMI-pH completed and the corrections calculated, we decided to further test the precision and relative accuracy of the SAMI-pH in lab. Both of the performance characteristics were determined in the experiment described below.

A sample collected from the Clark Fork River was transported back to the lab where it was immediately filtered and equilibrated with atmospheric CO_2. After filtration the water was transferred into a reagent bag. The reagent bag was then attached to the SAMI-pH, where the tests were run at room temperature (25.0 °C). The instrument flushed the plumbing and collected intensities for blank constants and then ran 12 pH

measurement cycles. The water that remained in the collection bottle after filling the reagent bag was used to collect pH measurements on the UV-VIS. The data for the SAMI-pH and UV-VIS resulted in a pH of 8.505 ±0.003 pH (N = 12) units and 8.499 ±0.005 pH units (N = 2), respectively a relative accuracy of -0.006 pH units. Another trial from a different grab sample obtained relative accuracy of a -0.001 pH units.

Samples were also transferred into a reagent bag without filtering or equilibration with atmospheric CO_2. The reagent bag was attached to the SAMI-pH, which was covered with a temperature-controlled chamber (this is to have a constant control over the temperature of the indicator reservoir and the sample water). The internal compartment of the chamber was then equilibrated to a temperature of 15°C. Once the desired temperature was achieved, the SAMI-pH ran 16 pH measurement cycles and a blank measurement cycle.

The calculated pHs from the 16 cycles were plotted versus the total indicator concentration (Figure 4.6). The calculated pH over the range of indicator concentrations was very reproducible for the multiple cycles (Figure 4.6A). As the indicator becomes more dilute (< 4.0E-6 M) the pH begins to scatter, which is due to the low absorbance measurements being within the noise of the instrument. For each measurement cycle, a single pH was collected with an indicator concentration as close to 6.0E-6 M as possible (Figure 4.6B). The average of the 16 single points resulted in an average pH of 8.607 with a precision of ±0.003 pH units.

The water that remained in the discrete sample bottle after the reagent bag was filled was analyzed by the UV-VIS spectrophotometer (Varian, Cary Bio 300) at a temperature of 15.0 °C. There were three total measurements made on the UV-VIS, one
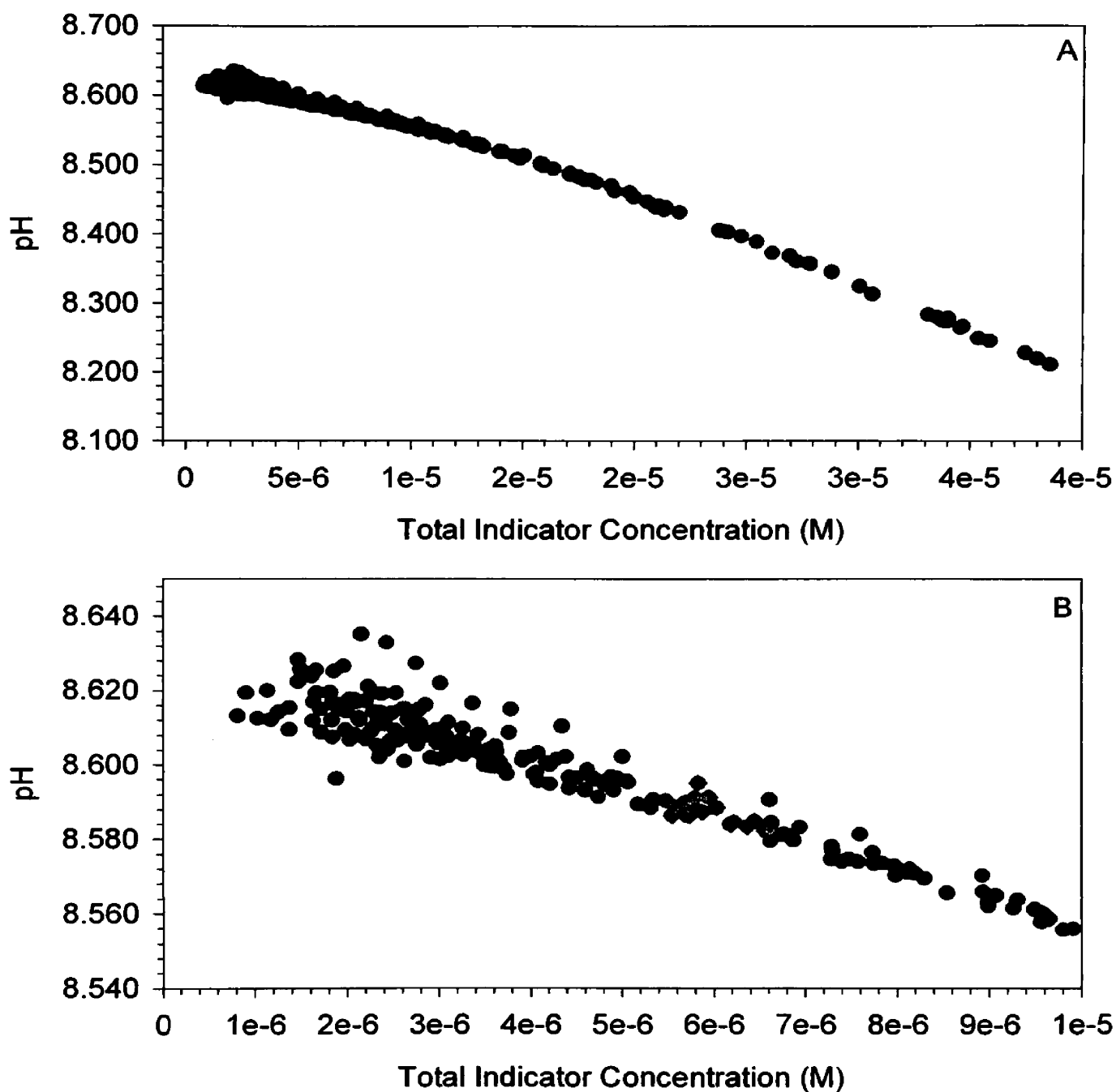
Figure 4.6. Over the full range of indicator concentration the pH is very reproducible for the 16 different pH measurement cycles (A). The average pH and standard deviation for the 16 cycles was 8.588 ±0.003 pH units (◆). The absorbance range for the 439 and 577 nm was 0.1140 to 0.1356 a.u. and 0.4354 to 0.5136 a.u., respectively.

from the bottle and two from the reagent bag. The tests resulted in a pH of 8.6813 ±0.002 pH units. With all the offsets applied the relative accuracy was determined to be 0.07 pH units. This trial will be discussed later.

4.3. Third Deployment

With the improvements made to the SAMI-pH operation a third deployment was scheduled. A longer deployment was still needed to test the long-term stability of the instrument. It would also enable more discrete samples to be collected, which would be used to investigate relative accuracy discrepancies between the first and second deployment. The third trial would also involve the collection of water samples to determine alkalinity.

The SAMI-pH was put back in the river, near the Sha-Ron fishing access (marked B in Figure 3.14), for a third time on October 25, 2000 and recovered November 3, 2000. The instrument was periodically retrieved from the river (on year day 300, 301, and 303) to download the data. After all corrections were applied to the data, temperature, I_{735}, and pH were then plotted versus Year Day (Figure 4.7).

The temperature measured with the portable temperature probe for the discrete samples was in good agreement with the autonomous instrument (Figure 4.7A). A plausible reason for the difference in the temperatures for the first two deployments was concluded after closer inspection of the river. The stretch of the river, where the SAMI-pH was deployed, had two distinctly different sections of water. One section was from
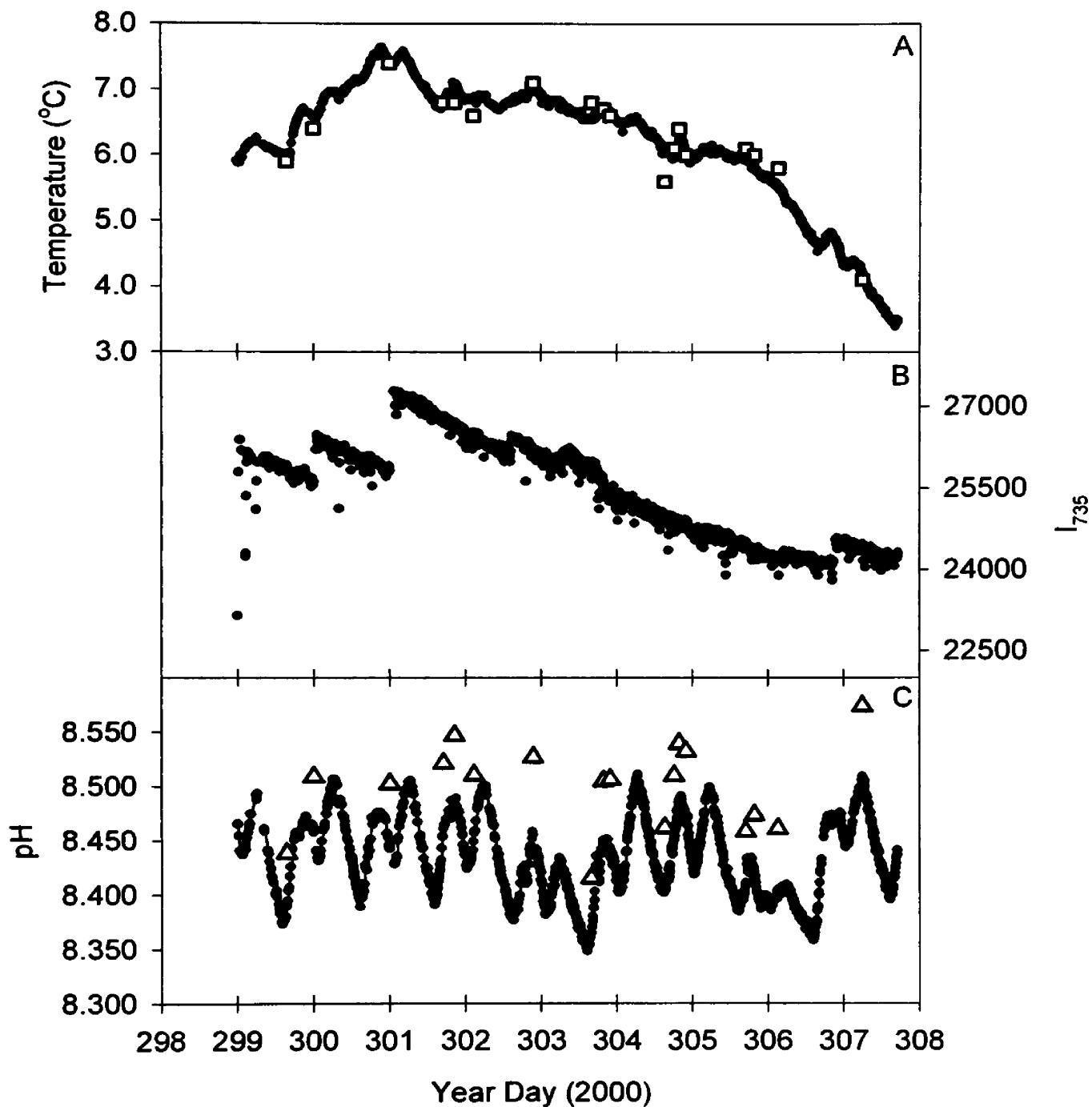
Figure 4.7. The third deployment data of the SAMI-pH, with temperature (□) and pH (△) from the discrete samples.

an eddy source, while the second represented the main part of the river. The temperature probe was tested in both sections of the river and it was verified that a temperature gradient was present between the two sections.

The I_{735} over the test period demonstrated a similar dependence on temperature as was observed in the prior deployments (Figure 4.7B). Two major intensity fluctuations year day 300 and 301 in the data were caused by the retrieval of the instruments.

The comparison of the corrected pH data from the discrete samples and the SAMI-pH resulted in a similar difference to the second deployment (Figure 4.7C). The average relative accuracy during the testing period was 0.041 pH units with a standard deviation of ±0.005 pH units (N = 18). The average alkalinity over the deployment was found to be 2775 ±30 μM. With the alkalinity well above the 2250 μM concentration it can be concluded that perturbation variability is not a major source of error in the relative accuracy.

The longer duration of the third deployment allowed for more discrete sample comparisons. By plotting the difference between the UV-VIS and the SAMI-pH over the duration of the deployment gives an indication if the instrument had drifted (Figure 4.8). Over the deployment error in the difference between the two methods was very systematic, ±0.005 pH units. This implies that instrument performance was stable and drift free over the extended period of time.
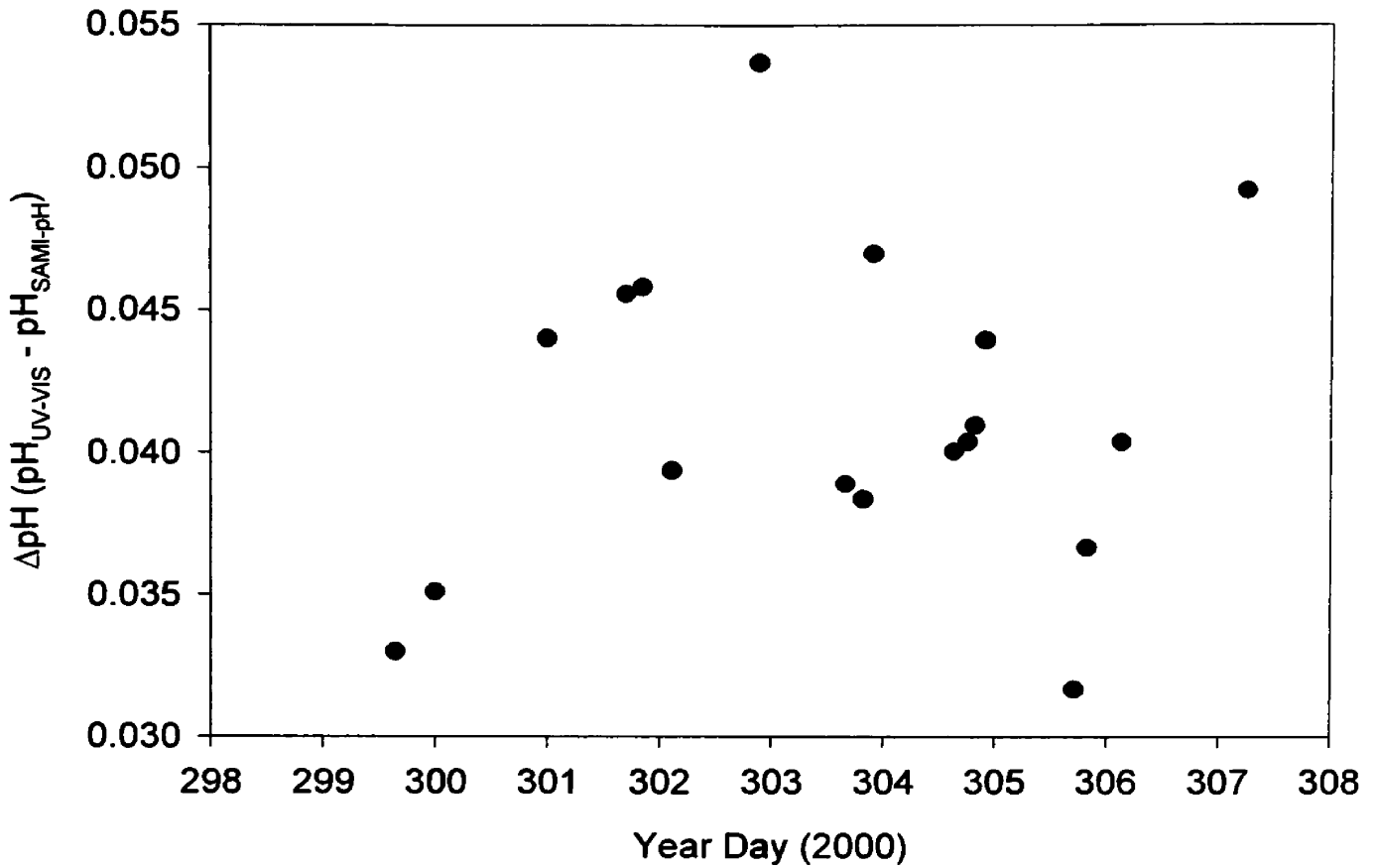
Figure 4.8. The SAMI-pH long-term stability over the duration of the October 2000 deployment, achieving an average relative accuracy of 0.041 pH units and a standard deviation about the mean of ±0.005 pH units (N = 18).

Chapter 5

Discussion and Conclusion

5.1 Discussion

5.1.a Summary of the River Deployments

Comparisons of pH versus year day for the three deployments yield a very noticeable difference in the magnitude of the diel cycles. The first deployment (near The University of Montana, Figure 3.14) resulted in a magnitude change of ~0.250 pH units while the second and third deployments (near the Sha-Ron fishing access, Figure 3.14) were ~0.150 and 0.135 units, respectively. Jason Reynolds, who deployed pCO_2 instrumentation at each of the sites to collect time series data, also documented a difference in the diel magnitude of pCO_2 between the two sites. The range was also found to be more variable at the downstream site.

Diel variability of the SAMI-pH and SAMI-CO_2 corresponded very well over the deployment times. If instrumental drift had occurred, there would have been a noticeable deviation in the inverse relationship between the SAMI-pH and pCO_2 instrumentation (Figure 4.2 and 4.7). Also, when all corrections were applied (including the correction for perturbation to zero indicator concentration) to the December 1999 data, there was a reduction from ~0.100 to ~0.055 pH units between the calculated and measured pH (Figure 5.1A).

70
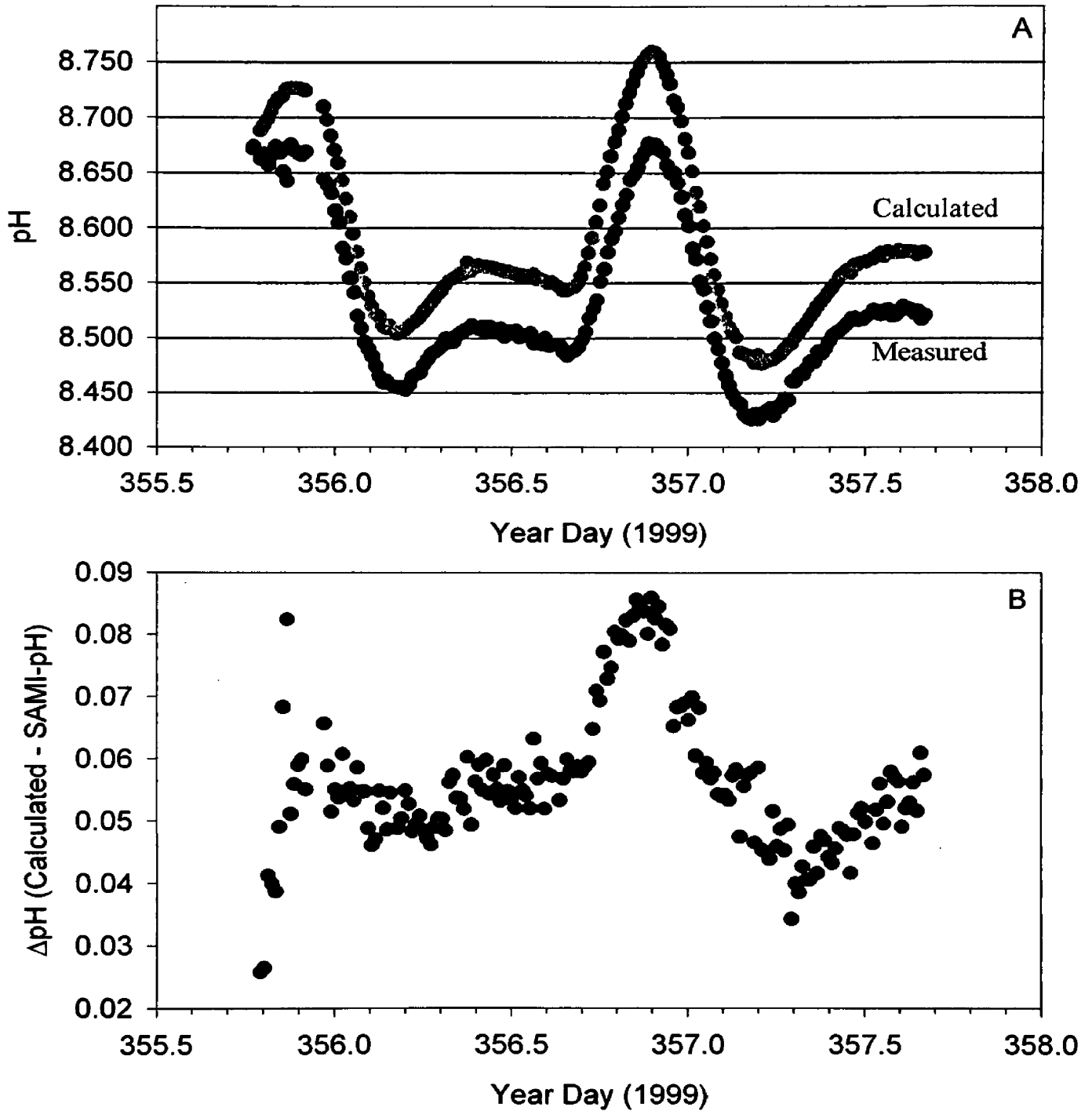
Figure 5.1. The corrected in situ and calculated pH for the December 1999 data (A) and the differences between the two data sets (B).

The observed difference in the two different methods is due to discrepancies in the determination of the $pK_a{}'$, the calculation of pH using the FRESHH2O.BAS program, and instrument responses times. When the $pK_a{}'$ was determined, a buffer of higher ionic strength (0.01 M) than the Clark Fork River (<0.005 M) was used. This caused the SAMI-pH to underestimate the "true" pH of the river. The calculated pH on the other hand overestimated the pH because it used equilibrium constants at infinite dilution or zero ionic strength. The variability in the difference plot is caused by response time differences between the two instruments (Figure 5.1B). Although there is variability I the data as previously mention, there is no observed instrumental drift. This demonstrates that it is stable over time. The SAMI-pH also proved to be a very stable and robust instrument during the third deployment when it taken out of the river (for a minimum of ½ hr.) three separate times to download the data (Figure 4.7). When the instrument was placed back into the river the pH data did not show any offset caused by the removal.

5.1.b Overview of SAMI-pH Performance

The SAMI-pH has attained all but one of the many operational standards set at the beginning of the research period (Table 5.1). It has demonstrated a precision of ±0.005 pH units, good long-term stability and freedom from drift, low power requirement (allowing for longer in situ duration), minimal indicator usage, and rapid response time (~ 2 minutes). The only shortfall of the autonomous instrument was the relative accuracy when compared to the UV-VIS.

The average relative accuracy of the three trials was -0.001, 0.029, and 0.041 pH units. If pH and alkalinity were used to determine pCO_2, these pH errors would result in

errors of ± 19, ± 57, and ± 89 µatms in the calculated $p\mathrm{CO}_2$. Although the SAMI-pH did

not attain the desired relative accuracy of better than ± 0.01 pH units for all of the

deployments, it has still outperformed an electrode. Electrodes have proven to be

unreliable for freshwater pH measurements, producing an uncertainty of ± 0.1 pH units

(Maberly 1996). An error of ± 0.1 pH units in pH measurements leads to an uncertainty

of ± 173 µatms in $p\mathrm{CO}_2$ calculations. As demonstrated earlier, the diurnal variability of

$p\mathrm{CO}_2$ in the Clark Fork River was only 230 µatms, so the error associated with a single

pH measurement would result in 75% of the total variability in the river $p\mathrm{CO}_2$

concentration.

The overall accuracy, which was determined by taking the difference of the

calculated pH (derived from $p\mathrm{CO}_2$ and alkalinity) and the pH from the SAMI-pH, was

reported as ~0.1 pH units. After correction for the SAMI-pH were made for perturbation

and molar absorptivity, the overall accuracy was reduced to ~0.06 pH units. This

discrepancy between the calculated and in situ data is caused by the differences in ionic

strength when pH is determined using the FRESHH2O.BAS program and the SAMI-pH

(uncertainty is in the pK_a' determination of cresol red). The program assumes that the

ionic strength of the river is at infinite dilution ($\mu = 0.000$ M) and the pK_a' was

determined in an ionic strength of 0.01 M. Since the ionic strength of the river is <0.005

M, the SAMI-pH will compute a pH of the river that is underestimated while the program

will overestimate the true pH of the river.

Table 5.1. Optimal response characteristics.

Characteristic	Description	Result
Dynamic Range	The working range of the indicator (Determined assuming an absorbance minimum of 0.1 and a maximum indicator concentration of 6.5x10^{-6} M, at 10 °C)	7.61 – 8.73 pH units
Response Time	Time required to detect 90% of a pH change	~ 2 minutes
Flush Time	Time required to completely flush the indicator from the plumbing	~ 5 minutes
Indicator Consumption	50 µL per pH measurement cycle (assuming 30 minute cycle interval)	73 mL of 0.020 mole kg^{-1} CR month^{-1}
Relative Accuracy	The agreement between the UV-VIS and SAMI-pH	0.041 ±0.005 pH units
Precision	The reproducibility for a single sample	Better than ±0.005 pH units
Power Limit	The length of deployment (assuming 2 measurement cycles per hour)	~ 1 month

As previously stated, the dynamics of the river at the two study sites were distinctly different. The study site near the University was more uniform (i.e. without rapids or eddies). At the upstream site (at Sha-Ron fishing access) there were rapids and eddies just above (~50 m) the deployment site along with eddies below the instrument. Although this may be a possible source of error when discrete samples were collected, it cannot be statistically verified because few relative accuracy tests were performed in the lab and in the field.

Comparisons of lab tests between unmodified river water and samples that had been filtered and equilibrated with atmospheric CO_2 demonstrates that there is a possible source of error caused by the composition of the river water. Although there is evidence of a difference between the experiments, the data can not be used to assess the difference in the various deployments due to few sample tests.

5.2 Conclusion

The relative accuracy of the instrument is an important issue that needs to be addressed so that the SAMI-pH can be used in further characterization of the carbonate system. Extensive lab testing using solutions of varying alkalinity and pCO_2 (this would control the pH) could be used to verify the overall and relative accuracy of the SAMI-pH. River samples that have been filtered and equilibrated with atmospheric CO_2 should also be thoroughly investigated against unmodified samples to ensure that the composition of the river is not a factor in the relative accuracy. The overall accuracy of the instrument could also be greatly enhanced if the pK_a' was determined using a low ionic strength

medium or at infinite dilution. A notable difference in the dynamics of the deployment sites necessitates more deployments to determine the possible source of error in the relative accuracy.

With improvements in electrical and instrumentation technology, the operation of the SAMI-pH can be enhanced. For example, a new low power data logger (Onset Computer Corporation) would decrease power consumption and increase the deployment duration of the instrument. The use of liquid core wave-guides would increase the optical pathlength, thereby reducing indicator concentrations and pH perturbation. The optical bandpass of the SAMI-pH could be improved by replacing the holographic grating with a photodiode/filter combination (Intor Corp.). And finally, for the SAMI-pH to be used in a system that experiences large fluctuations in pH, like acid mine drainage, multiple indicator solutions could be characterized and used to detect wide ranges of pH.

In combination with pCO$_2$ instrumentation, the SAMI-pH would be beneficial in collecting long-term time series data for determining diel, episodic, and seasonal trends of the carbonate parameters. With these improvements and the combination of other in situ instrumentation a better understanding of the cycling

Appendix I

SAMI-pH Operating Program (pHV3.TT4)

```
DIM(128,4096)
  1 REM =-=-=-=-=-=-=-=-=-pHV3.TT4=-=-=-=-=-=-=-=-=-=-=-=-=.
  3 REM SAMI-pH SENSOR CONTROL (VERSION 3)
  4 REM MODIFIED OCTOBER 25, 2000  BY JEFF CARR
  5 REM =-=-=-=-=-=-=-=-=-=-=-=-=-=-=-=-=-=-=-=-=-=-=-=-=-=
 10 REM GOTO 2000 (DATA DUMP), 3000 (SET CLOCK, DATA COUNTER)
 15 REM I/O(0) = POWER        I/O(1) = LAMP
 20 REM I/O(2) = PUMP         I/O(3) = VALVE
 25 REM I/O(6) = DETECTOR +/- 12V SUPPLY
 30 REM CHAN(0) = 434 nm (RED)     CHAN(1) = 577 nm (GREEN)
 35 REM CHAN(3) = 740 nm (BLUE)    CHAN(7) = TEMPERATURE
 40 REM =-=-=-=-=-=-=-=-=-=-=-=-=-=-=-=-=-=-=-=-=-=-=-=-=-=
 50 ASM &H9B, DB 8 :REM 512K MEMORY EXPANSION
 60 PCLR 0,1,2,3: PSET 6 :REM SHUT OFF ALL DEVICES
 80 GOSUB 3000 : REM SET DATE AND TIME
 90 H = 1: GOTO 200: REM IF STARTING DON'T WAIT 1/2 HOUR
 99 REM =-=-=-=-=-=-=-=-=- CTRL-C DESTINATION -=-=-=-=-=-=-=-=-=.
100 PCLR 0,1,2,3: PSET 6
105 ASM &HBB,DB &H0A:C = CHAN(0)
110 STOP
200 REM =-=-=-=-=-=-=-= START OF MEASUREMENT SEQUENCE -=-=-=-=-=-=.
210 U = U + 1: IF U >= 96 GOTO 350: REM BLANK CYCLE COUNTER (USE 96 IF
    1/4 HR MEAS.)
215 IF H=1 GOTO 250
218 PCLR 0,1,2,3: PSET 6
230 GOSUB 6000: REM 15 MIN. WAIT LOOP
250 PCLR 0,1,2,3: PSET 6
255 H = 0
260 PSET 0
262 ASM &HBB,DB &H0E: REM TURNS ON DETECTOR POWER
264 C = CHAN(0)
266 PSET0: PCLR 6
268 SLEEP0:SLEEP 600
270 REM **** DARK SIGNAL AVERAGES ****
272 I = 0:J = 0: K = 0
274 FOR C = 1 TO 25
276 A = CHAN(0): B = CHAN(1): D = CHAN(2)
278 I =I + A: J = J + B: K = K + D
280 SLEEP 0: SLEEP 1
281 NEXT C
282 I = I/25: J = J/25: K = K/25
```

```
283 SLEEP0:SLEEP200
284 REM  **** TURN LAMP ON ****
285 PSET 1
286 FOR S=1 TO 10
287 PSET2: SLEEP0: SLEEP 100: PCLR2
288 SLEEP0:SLEEP100
290 NEXT S
292 REM ** SINGLE INDICATOR PULSE **
293 PSET 3: SLEEP 0: SLEEP 10
294 PSET 2: SLEEP 0: SLEEP100: PCLR 3
295 SLEEP 0: SLEEP 10: PCLR 2
296 REM ** NUMBER OF SAMPLE PULSES BEFORE MEASUREMENT **
297 FOR R = 1 TO 14
299 PSET 2: SLEEP 0: SLEEP100: PCLR 2
300 FOR S=1TO2
304 SLEEP 0: SLEEP 100
306 NEXT S
310 NEXT R
312 SLEEP0:SLEEP100
315 REM ** NUMBER OF MEASUREMENT CYCLES **
320 FOR P = 1 TO 18
325 GOSUB 1000
330 NEXT P
340 REM  **** SHUT OFF: LAMP, AMPS, V SWITCHED ****
342 PCLR 1: PSET 6: PCLR 0
344 C = CHAN(0)
346 ASM &HBB,DB &H0A
348 GOTO 200
350 REM =-=-=-=-=-=-=-=-= BLANK AND REAGENT FLUSH =-=-=-=-=-=-=-=-=
355 U =192
357 PSET 0
362 ASM &HBB,DB &H0E
364 C = CHAN(0)
366 PSET0: PCLR 6
368 SLEEP0:SLEEP 600
370 REM  **** DARK SIGNAL AVERAGES ****
372 I = 0:J = 0: K = 0
374 FOR C = 1 TO 25
376 A = CHAN(0): B = CHAN(1): D = CHAN(2)
378 I =I + A: J = J + B: K = K + D
380 SLEEP 0: SLEEP 1
381 NEXT C
382 I = I/25: J = J/25: K = K/25
383 SLEEP0:SLEEP200
384 REM  **** TURN LAMP ON ****
386 PSET 1
```

```
388 FOR S = 1 TO 82
390 PSET 2: SLEEP 0: SLEEP 100: PCLR 2:  REM  **** PUMP ****
470 REM -- WAIT 2 SECS --
480 FOR R = 1 TO 2
490 SLEEP 0: SLEEP 100
500 NEXT R
520 NEXT S
522 REM  **** GO TO MEASUREMENT ROUTINE ****
524 REM ASM &HBB,DB &H0E
525 REM C = CHAN(0)
527 REM PCLR 6
528 GOSUB 1000
530 GOSUB 1000
540 REM  **** SHUT OFF: LAMP, AMPS, V SWITCHED ****
542 PCLR 1: PSET 6: PCLR 0
544 C = CHAN(0)
546 ASM &HBB,DB &H0A
548 H=0:U = 0
549 REM **** INDICATOR PULSE TO FLUSH OUT BLANK ****
550 PSET 0
555 FOR S = 1 TO 2
560 PSET 3: SLEEP 0: SLEEP 10
565 PSET 2: SLEEP 0: SLEEP 100: PCLR 2
570 SLEEP 0: SLEEP 100: PCLR 3
580 FOR R = 1 TO 2
585 SLEEP 0: SLEEP 100
590 NEXT R
600 FOR Q = 1 TO 10
605 PSET 2: SLEEP 0: SLEEP 100: PCLR 2
610 FOR R = 1 TO 2
615 SLEEP 0: SLEEP 100
620 NEXT R
625 NEXT Q
630 NEXT S
710 GOTO 200
1000 REM =-=-=-=-=-=-=-=-=- MEASUREMENT SEQUENCE =-=-=-=-=-=-=-=-=
1090 RTIME
1095 PRINT "*************************************************"
1100 PRINT #02, "CURRENT TIME = ",?(2),":",?(1),":",?(0);
1105 PRINT #02, " ON ",?(4),"/",?(3),"/",?(5)
1107 G = CHAN(7)
1111 PRINT #04, "TEMPERATURE = ",TEMP(G)
1112 PRINT "434 nm  577 nm  740 nm"
1115 STORE X,#2,?(2),?(1),?(0)
1117 STORE X,#2,?(4),?(3),?(5)
1119 STORE X,#2,G
```

```
1155 Y=0
1160 IF U >=192 Y=2222
1176 PRINT #5,"   BLANK COUNTER",Y
1178 STORE X,#2,Y
1170 PRINT #5,"DARK SIGNALS", I," ",J," ",K
1280 PSET 2: SLEEP 0: SLEEP 100: PCLR 2
1290 SLEEP 0: SLEEP 100
1344 REM **** LIGHT SIGNALS ****
1360 T = 0: F = 0: V = 0
1365 FOR C = 1 TO 25
1370 A = CHAN(0): B = CHAN(1): D = CHAN(2)
1375 T = T + A: F = F + B: V = V + D
1380 SLEEP 0: SLEEP 1
1385 NEXT C
1390 T = (T/25-I): F = (F/25-J): V = (V/25-K)
1395 PRINT #5,T," ",F," ",V
1465 STORE X,#2,T,F,V
1466 REM PCLR1
1547 SLEEP 0: SLEEP 100
1548 REM **** SHUT OFF: LAMP, AMPS, V SWITCHED ****
1550 REM PCLR 1: PSET 6: PCLR 0
1552 REM C = CHAN(0)
1564 REM ASM &HBB,DB &H0A
1549 RETURN
1999 =.=.=.=.=.=.=.=.=.=.=.= READ DATA FILE =.=.=.=.=.=.=.=.=.=.=.
2000 FOR W = 1 TO (X/22)
2010 IF W = 1  X = 0
2015 PRINT #02,GET(X,#2),":",GET(X,#2),":",GET(X,#2)," ";
2025 PRINT #02,GET(X,#2),"/",GET(X,#2),"/",GET(X,#2)," ";
2030 Y=GET(X,#2)
2031 PRINT #5,TEMP(Y)," ";
2032 Y=GET(X,#2)
2034 IF Y = 0 GOTO 2038
2036 PRINT "BLANK"," ";
2037 GOTO 2040
2038 PRINT "*****"," ";
2040 PRINT #5,GET(X,#2)," ",GET(X,#2)," ",GET(X,#2)
2062 SLEEP 0 : SLEEP 10
2065 NEXT W
2070 STOP
3000 REM =.=.=.=.=.=.=.=.=.=.= SET TIME AND DATE =.=.=.=.=.=.=.=.=
3010 INPUT 'ENTER YEAR   (0 - 99) '?(5)
3020 INPUT 'ENTER MONTH  (1 - 12) '?(4)
3030 INPUT 'ENTER DAY    (1 - 31) '?(3)
3040 INPUT 'ENTER HOUR   (0 - 23) '?(2)
3050 INPUT 'ENTER MINUTE (0 - 59) '?(1)
```

```
3060 INPUT 'ENTER SECOND (0 - 59) '?(0)
3070 STIME
3080 RETURN
6000 REM =-=-=-=-=-=-=- WAIT FOR NEXT WHOLE HALF HOUR =-=-=-=-=-=-
6005 RTIME
6007 IF ?(1) < 10 Z = 15: GOTO 6040
6010 IF ?(1) < 25 Z = 30: GOTO 6040
6015 IF ?(1) < 40 Z = 45: GOTO 6040
6020 IF ?(1) < 55 Z = 0: GOTO 6040
6040 SLEEP 0: SLEEP 500
6050 RTIME
6060 IF ?(1) <> Z GOTO 6040
6070 RETURN
```

References

ANDREW, K. N., BLUNDELL, N. J., PRICE, D., AND P. J. WORSFOLD. 1994. On-site automated FI monitors provide near-continuous, reliable, and low-cost data for assessing water quality. Analytical Chemistry, **66**: 917A-922A

ANGEL, S. M., GARVIS, D. G., SHARMA, S. K., A. SEKI. 1989. Field applications of fiber-optic sensors. Part I: Temperature measurements in a geothermal well. Applied Spectroscopy, **43**: 430-435.

BAUMANN, E. W. AND B. R. BUCHANAN. 1991. Colorimetric pH determination with computer modeling. Applied Spectroscopy, **45**: 632-636.

BELLERBY, R. G. J., G. E. MILLWARD, D. R. TURNER AND P. J.WORSFOLD 1993. Approaches to the continuous monitoring of seawater pH and its role in the global carbon cycle. Trends in Analytical Chemistry, **12**(9): 382-386.

BELLERBY, R. G. J., D. R. TURNER, G. E. MILLWARD, AND P. J. WORSFOLD. 1995. Shipboard flow injection determination of sea water pH with spectrophotometric detection. Analytica Chimica Acta, **309**: 259-270.

BEN-YAAKOV, S. AND E. RUTH. 1973. An improved in situ pH sensor for oceanographic and limnological applications. Dept. of Geology. UCLA, Los Angeles 90024. *Notes*. 144-151.

BREZINSKI D. P. 1983. Kinetic, Static and stirring errors of liquid junction reference electrodes. The Analyst, **109**: 425-442

BRICK, C. M. AND J. N. MOORE. 1996. Diel variation of trace metals in the upper Clark Fork River, Montana. Environmental Science and Technology, **30**(6): 1953-1960.

BROWN, W. E. BROWN AND J. A. CAMPBELL. 1968. Acid-base indicator: An experiment in aqueous equilibria. Journal of Chemical Education, **45**: 674-675.

BYRNE, R. H., W. YAO, E. KALTENBACHER, AND R. D. WATERBURY. 2000. Construction of a compact spectrofluorometer/spectrophotometer system using a flexible liquid core waveguide. Talanta, **50**:1307-1312.

BYRNE, R.H., S. MCELLIOT, R. A. FEELY, F. J. MILLERO. 1999. The role of pH$_T$ in marine CO$_2$-system characterizations. Deep Sea Research I, **46**: 1985-1997.

BYRNE, R. H., WATERBURY, R. D., KELLY, J. J., LEADER, B., RUSSELL, R., JONES, C. W., KOLESAR, J, R., AND S. MCELLIGOTT. 1999. Apparatus and method for in situ pH measurements of aqueous medium. Patent US5925572.

BYRNE, R.H., E. KALTENBACHER, AND R. WATERBURY. 1999. Autonomous *in-situ* analysis of the upper ocean. 1999. Sea Technology: 71-75.BYRNE, R. H. AND J. A. BRELAND. 1989. High precision multiwavelength pH determinations in seawater using cresol red. Deep-Sea Research, 36(5): 803-810.

BYRNE, R. H. R. H., G. ROBERT-BALDO, S. W. THOMPSON, AND C.T.A.CHEN. 1988. Seawater pH measurements: an at-sea comparison of spectrophotometric and potentiometric methods. Deep-Sea Research, 35: 1405-1410.

BYRNE, R. H. 1987. Standardization of standard buffers by visible spectrometry. Analytical Chemistry, 59: 1479-1481.

CLAYTON, T. D. AND R. H. BYRNE. 1993. Spectrophotometric seawater pH measurements: total hydrogen ion concentration scale calibration of *m*-cresol purple and at-sea results. Deep-Sea Research, 40: 2115-2129.

CLAYTON, T. D., R. H. BYRNE, J. A. BRELAND, R. A. FREELY, F. J. MILLERO, D. M. CAMPBELL, P. P. MURPHY, AND M. F. LAMB. 1995. The role of pH measurements in moderate oceanic CO_2-system characterizations: Precision and thermodynamic consistency. Deep-Sea Research, 42: 411-429

COVINGTON, A. K., R. G. BATES AND R. A. DURST. 1985. Definition of pH scales, standard reference values, measurement of pH and related terminology. Pure & Applied Chemistry, 57: 531-542.

COVINGTON, A. K., P. D. WHALLEY AND W. DAVISON. 1983. Procedures for the measurement of pH in low ionic strength solutions including freshwater. Analyst, 108: 1528-1532.

COVINGTON, A. K. 1981. Recent developments in pH standardization and measurement for dilute aqueous solutions. Analytica Chimica Acta, 127: 1-21.

DAVISON, W., AND C. WOOF. 1985. Performance tests for the measurements of pH with glass electrodes in low ionic strength solutions including natural waters. Analytical Chemistry, 57: 2567-2570.

DEGRANDPRE, M. D. 1999. Development of a stable, high resolution, autonomous pH monitoring system for freshwater applications. Grant

DEGRANDPRE, M. D., HAMMAR, T. R., WALLACE, W. R. AND C. D. WIRICK. 1997. Simultaneous mooring-based measurments of seawater CO2 and O2 off Cape Hatters, North Carolina. Limnology and Oceanography, 42 (1): 21-28.

FRENCH, C. M., DEGRANDPRE, M. D., CARR, J. J., DOUGHERTY, E., EIDSON, L. A. K. AND J. REYNOLDS. 2000. Spectrophotometric pH measurements of freshwater. Submitted to Analytica Chimica Acta.

FRENCH, C. M. 1999. EVALUATION OF SPECTROPHOTOMETRIC PH METHODS FOR FRESHWATER MEASUREMENTS. M.S. THESIS, UNIVERSITY OF MONTANA-MISSOULA.

GARDNER, M. J., J. E. RAVENSCROFT, AND C. ACKERS. 1997. Control samples for the determination of pH in low ionic strength waters: consensus values from interlaboratory tests. Talanta, 44: 111-117.

GARDNER, M. J., R. GILL AND J. E. RAVENSCROFT. 1990. Control samples for pH determination in low ionic strength waters. Analyst, 115: 371-374.

HAINES, T. A., J. J. AKIELASZEK, S. A. NORTON AND R. B. DAVIS. 1983. Errors in pH measurement with colorimetric indicators in low alkalinity waters. Hydrobiologia, 107: 57-61.

HALES, B., BURGESS, L., AND S. EMERSON. 1997. An absorbance-based fiber-optic sensor for $CO_{2(aq)}$ measurement in porewaters of sea floor sediments. Marine Chemistry, 59: 51-62.

HARBINSON, T. R. AND W. DAVISON. 1987. Performance of flowing and quiescent free-diffusion junctions in potentiometric measurements at low ionic strengths. Analytical Chemistry, 59: 2450-2456.

HARRIS, D. C. 1982. Quantitative Chemical Analysis, 2nd ed. W. H. Freeman and Company, New York, 92.

HENRIKSEN, A. 1979. A simple approach for identifying and measuring acidification of freshwater. Nature, 278: 542-545.

HERCZEG, A. L., W. S. BROECKER, R. F. ANDERSON, S. L. SCHIFF AND D. W. SCHINDLER. 1985. A new method for monitoring temporal trends in acidity of fresh waters. Nature, 315: 133-135.

HEONICKE, R., M. A. STAPANIAN, L. J. ARNET, AND R. C. METCALF. 1991. Consequences of pH measurement errors. Freshwater Biology, 25: 261-278.

HERCZEG, A. L. AND R. H. HESSLEIN. 1984. Determination of hydrogen ion concentration in softwater lakes using carbon dioxide equilibria. Geochimie Cosmochimie Acta, 48: 837-845.

INGLE, J. D. AND S. R. CROUCH. 1988. Spectrochemical Analysis. Prantice-Hall, Inc.: New Jersy.

JANATA, J., JOSOWICZ, M., AND D. M. DEVANE. 1994. Chemical sensors. Analytical Chemistry, **66**: 207R-228R.

JANNASCH, H. W., JOHNSON, K. S., AND C. M. SAKAMOTO. 1994. Submersible, osmotically pumped analyzers for continuous determination of nitrate in situ. Analytical Chemistry, **66**: 3352-3361.

KING, D.W. AND D. R. KESTER. 1990. Spectral Modeling of Sulfonephthalein indicators: Application to pH measurements using multiple indicators. Applied Spectroscopy, **44**: 722-727.

KING, D. W. AND D. K. KESTER. 1989. Determination of seawater pH from 1.5 to 8.5 using colorimetric indicators. Marine Chemistry, **26**: 5-20.

KOCK, W. F., MARINENKO, G., AND R. C. PAULE. 1985. An Interlaboratory Test of pH Measurements in Rainwater. Journal of Research of the National Bureau of Standards, **91**: 23-31

KOLB, C. E., WORMHOUDT, J. C., M. S. ZAHNISER. 1995. Recent advances in spectroscopic instrumentation for measuring stable gases in the natural environment. Biogenic Trace Gases. Matson and Harris ed. Blackwell Sciences

KOLTHOFF, I. M. 1928. The "salt error" of indicators in colorimetric determination of pH. Journal of Physical Chemistry, **32**: 1820-1833.

KOLTHOFF, I. M. 1930. Indicator Constants. Journal of Physical Chemistry, **34**: 1466-1483.

KOPELOVE, A., S. FRANKLIN, AND G. M. MILLER. 1989. Low ionic strength pH measurement. American Laboratory, **21**: 40-47.

KRAMER, J. AND A. TESSIER. 1982. Acidification of aquatic systems: a critique of chemical approaches. Environmental Science and Technology, **16**(11): 606A-615A.

LEWIS, E., AND D. W. R. WALLACE. 1998. Program developed for CO_2 system calculations. ORNL/CDIAC-105. Carbon Dioxide Information Analysis Center, Oak Ridge National Laboratory, U.S. Department of Energy, Oak Ridge, Tennessee.

MABERLY, S. C. 1996. Diel, episodic and seasonal changes in pH and concentrations of inorganic carbon in a productive lake. Freshwater Biology, **35**: 579-598.

MACKEY, D. J., BUTTLER, E. C. D., NICOLS, P. D., H. W. HIGGINS 1989. Continuous shipboard and in situ measurements of pH and fluorescence in seawater. Marine Chemistry, **28**: 41-60

MIDGELY, D. 1987. Assessment of reference electrodes for use in determining the pH of acidic, poorly-buffered waters. Atmospheric Environment, **21**: 173-177.

MILLERO, F. J. 1986. The pH of estuarine waters. Limnology and Oceanography, **31**: 839-847

MILLERO, F. J., J. ZHANG, S. FIOL, S. SOTOLONGO, R.N. ROY, K. LEE, AND S. MANE. 1993. The use of buffers to measure the pH of seawater. Marine Chemistry, **44**: 143-152

MIZAIKOFF, D., JAKUSCH, M., AND M. KRAFT. 1999. Infrared fiber-optic sensors-Versatile tool for water monitoring. Sea Technology: 25-34

MOTELLIER, M., H. MICHELS, B. DUREAULT, AND P. TOULHOAT. 1993. Fiber-optic sensor for *in situ* applications. Sensors and Actuators, **11**: 467-473

OZEKI, T., Y. TANAKA, M. FUKAMIZU, AND N. OGAWA. 1999. Plots of the pH *versus* electric conductivity of rainwater for evaluating the accuracy of pH measurements. Analytical Science, **15**: 1159-1161.

OZEKI, T., Y. TSUBOSAKA, S. NAKAYAMA, N. OGAWA, AND T. KIMOTO. 1998. Study of errors in determination of hydrogen ion concentrations in rainwater samples using glass electrode method. Analytical Science, **14**: 749-756.

PEAK, D. V. AND R. C. METCALF. 1991. Dilute, neutral pH standard of known conductivity and acid neutralizing capacity. Analyst, **116**: 221-231

PIA, S. H., D. P. WALTMAN, D. C. HILLMAN AND K. W. STREET, JR. 1990. Spectrophotometric determination of pH by flow injection. Analytica Chimica Acta, **231**: 21-26.

PINOL, P., AND A. AVILA. 1992. Streamwater pH, alkalinity, $p\text{CO}_2$ and discharge relationships in some forested Mediterranean catchments. Journal of Hydrology, **131**: 205-225

RAMETTE, R. W., C. H. CULBERSON AND R. G. BATES. 1977. Acid-base properties of tris(hydroxymethyl)aminomethane (tris) buffers in seawater from 5 to 40 °C. Analytical Chemistry, **48**: 867-870.

RANALLI, A. J. 1998. An evaluation of in-situ measurements of water temperature, specific conductance, and pH in low ionic strength streams. Water, Air, Soil Pollution, **104**: 423-441.

ROBERT-BALDO, G. L., M. J. MORRIS, AND R. H. BYRNE. 1985. Spectrophotometric determination of seawater pH using phenol red. Analytical Chemistry, 57: 2564-2567.

ROGERS, K. M., AND E. J. POZIOMEK. 1996. Fiber optic sensors for environmental monitoring. Chemosphere, 33: 1151-1174.

SEDJIL, M., AND G. N. LU. 1998. A seawater pH determination method using a BDJ detector. Measurement Science Technology, 9: 1587-1592.

SEDJIL, M., G. N. LU, G. MICHARD, AND F. PREVOT. 1998. A colorimetric method with the use of BDJ detector for seawater pH measurement. Analytica Chimica Acta, 377: 179-184.

SERRA, G., A. SCHIRONE AND R. BONIFORTI. 1990. Fibre-optic pH sensor for sea-water monitoring using a single dye. Analytica Chimica Acta, 232: 337-344.

STAUFFER, R. E. 1990a. Alkalinities of Maine lakes: are they really changing? Limnology and Oceanography, 35(6): 1238-1257.

STAUFFER, R. E. 1990b. Electrode pH error, seasonal epilimnetic pCO$_2$, and the recent acidification of the Maine lakes. Water Air Soil Pollution, 50: 123-148.

STUMM, W., AND J. J. MORGAN. 1996. Aquatic Chemistry: Chemical Equilibria and Rates in Natural Waters. 3rd ed. John Wiley & Sons, Inc., New York.

WATERBURY, R. D., R. H. BYRNE, J. KELLY, B. LEADER, S. MCELLIGOTT AND R. RUSSELL. 1996. Development of an underwater in-$situ$ spectrophotometric sensor for seawater pH. SPIE, 2836: 170-177.

YAMAZAKI, H. R.P. SPERLINE, AND H. FREISER. 1992. Spectrophotometric determination of pH and its application to determination of thermodynamic equilibrium constants. Analytical Chemistry, 64: 2720-2725

ZHANG, H. AND R. H. BYRNE. 1996. Spectrophotometric pH measurements of surface seawater at in-situ conditions: absorbance and protonation behavior of thymol blue. Marine Chemistry, 52: 17-25.